

Efficient numerical computation of time-fractional nonlinear Schrödinger equations in unbounded domain

Jiwei Zhang, Dongfang Li, Xavier Antoine

► **To cite this version:**

Jiwei Zhang, Dongfang Li, Xavier Antoine. Efficient numerical computation of time-fractional nonlinear Schrödinger equations in unbounded domain. *Communications in Computational Physics*, Global Science Press, 2019, 25 (1), pp.218-243. 10.4208/cicp.OA-2017-0195 . hal-01422725

HAL Id: hal-01422725

<https://hal.archives-ouvertes.fr/hal-01422725>

Submitted on 26 Dec 2016

HAL is a multi-disciplinary open access archive for the deposit and dissemination of scientific research documents, whether they are published or not. The documents may come from teaching and research institutions in France or abroad, or from public or private research centers.

L'archive ouverte pluridisciplinaire **HAL**, est destinée au dépôt et à la diffusion de documents scientifiques de niveau recherche, publiés ou non, émanant des établissements d'enseignement et de recherche français ou étrangers, des laboratoires publics ou privés.

Efficient numerical computation of time-fractional nonlinear Schrödinger equations in unbounded domain

Jiwei Zhang ^{*} Dongfang Li[†] Xavier Antoine[‡]

December 26, 2016

Abstract

The aim of this paper is to derive an efficient scheme for solving one-dimensional time-fractional nonlinear Schrödinger equations set in unbounded domains. We first derive some absorbing boundary conditions for the fractional system by using the unified approach introduced in [57, 58] and a linearization procedure. Then, the initial boundary-value problem for the fractional system with ABCs is discretized and the error estimate $\mathcal{O}(h^2 + \tau)$ is stated. To accelerate the scheme in time, the fractional derivative is approximated through a linearized L1-scheme. Finally, we end the paper by some numerical simulations to validate the properties (accuracy and efficiency) of the derived scheme. In addition, we illustrate the behavior of the solution by reporting a few simulations for various parameter values of the fractional order $0 < \alpha < 1$, nonlinearities and potentials.

Contents

1	Introduction	2
2	Construction of nonlinear ABCs for the TFNSE	4
3	<i>A priori</i> error estimates	7
4	Discretization and analysis of the schemes	9
4.1	Derivation of the linearized L1-scheme	9
4.2	Numerical analysis of the linearized L1-scheme	11
4.3	Fast evaluation based on the L1-schemes	15
5	Numerical examples	17

^{*}Beijing Computational Science Research Center, Beijing 100094, China (jwzhang@csrc.ac.cn). The research of this author was supported by the National Natural Science Foundation of China under grant 91430216.

[†]School of Mathematics and Statistics, Huazhong University of Science and Technology, Wuhan 430074, China. (dfli@hust.edu.cn). The research of this author was supported by the National Natural Science Foundation of China under grants No. 11571128.

[‡]Institut Elie Cartan de Lorraine, UMR CNRS 7502, Université de Lorraine, Inria Nancy-Grand Est, SPHINX Team, F-54506 Vandoeuvre-lès-Nancy Cedex, France. (xavier.antoine@univ-lorraine.fr). The research of this author was supported by the French ANR grant Bond (ANR-13-BS01-0009-01) and the LIASFMA (funding from the University of Lorraine).

1 Introduction

The classical Schrödinger equation serves as the Feynman propagator for nonrelativistic quantum mechanics using a Gaussian probability distribution in the space of all possible paths. This provides a useful mechanism that accounts naturally for the non-Gaussian distributions corresponding to fractional structures. By extending the Feynman path integral from Gaussian distribution to Lévy-like quantum mechanical paths, Laskin proposed in [33–36] a space fractional Schrödinger equation, proved that the associated fractional Hamiltonian is hermitian and that the parity is conserved. Guo and Huo [24] stated the local well-posedness in subcritical space for the Cauchy problem of the nonlinear fractional Schrödinger equation. Kirkpatrick and Zhang studied the dynamics and observed the behavior of the decoherence and turbulence of the Schrödinger equation with a fractional Laplacian operator that can arise in some cases, and presented the results to be consistent with the long-range interactions. Ionescu *et al.* [42] considered the question of the global existence of a fractional semilinear cubic Schrödinger equation. Duo and Zhang [19] computed the ground and first excited states of fractional Schrödinger equations in an infinite potential well. In [7], the authors proposed a numerical study of the ground states and dynamics of space fractional rotating Gross-Pitaevskii equations with nonlocal interactions through pseudospectral approximation schemes.

Recently, Naber [45] built the Time Fractional Schrödinger Equation (TFSE) in analogy with the fractional Fokker-Planck equation as well as with the application of Wick rotation of time. Related works have next been developed [12, 18, 41, 46, 53], including the generalization of the TFSE to a full space and time fractional quantum dynamics version and some new results on the correct continuity equation for the probability density. The fractional nonlinear Schrödinger equation is used to describe the nonlocal quantum phenomena in quantum physics and explore the quantum behaviors of either long-range interactions or time-dependent processes with many scales. There are many applications to consider this new and fast developing part in quantum physics [31, 33–36, 41, 45, 46, 52, 55, 56]. Some analytical and approximate solutions have been considered for the TFSE [29, 48]. The complexity of the TFSE with different potentials and nonlinearities precludes detailed analytical studies of its non standard properties. Therefore, efficient and accurate numerical simulations [13, 22, 26, 44, 54] are urgently needed to understand them.

In this paper, we develop some efficient numerical methods for computing the solution to general 1D Time-Fractional Nonlinear Schrödinger Equations (TFNSE) given by

$$\begin{cases} i_0^C \mathcal{D}_t^\alpha \psi(x, t) = -\psi_{xx} + V(x)\psi + f(|\psi|^2)\psi, & (x, t) \in \mathbb{R} \times (0, T], \\ \psi(x, 0) = \psi_0(x), & x \in \mathbb{R}, \\ \psi(x, t) \rightarrow 0 \text{ when } |x| \rightarrow +\infty, & t \in (0, T], \end{cases} \quad (1.1)$$

where $i = \sqrt{-1}$ and $V(x)$ is the external potential function. The function f allows to include general nonlinear effects with respect to ψ , e.g. for the case of the cubic nonlinearity $f(|\psi|^2)\psi = g|\psi|^2\psi$ that arises in nonlinear optics. If $g = +1$, one gets the well-known *defocusing* nonlinearity while $g = -1$ corresponds to the *focusing* situation. The operator ${}_0^C \mathcal{D}_t^\alpha$ denotes the Caputo fractional derivative of order α ($0 < \alpha < 1$) with respect to t [59] and given by

$${}_0^C \mathcal{D}_t^\alpha \psi(x, t) = \frac{1}{\Gamma(1-\alpha)} \int_0^t \frac{1}{(t-s)^\alpha} \frac{\partial \psi(x, s)}{\partial s} ds, \quad 0 < \alpha < 1, \quad (1.2)$$

where Γ is the Gamma special function.

To numerically solve problem (1.1), there are three essential difficulties

- (1) the unboundedness of the spatial domain,
- (2) the nonlinearity f ,
- (3) and the huge storage and computational cost of the (nonlocal) Caputo derivative.

To overcome the first problem, the method of *Artificial/Absorbing Boundary Conditions* (ABCs) is a powerful way to reformulate the initial problem in the unbounded domain as another problem appropriately set in a bounded domain [1, 6, 25]. The basic idea is to build a suitable ABC to eliminate the waves striking a fictitious boundary introduced to bound the computational domain. In the literature, much attention has been received to study the construction of ABCs for time-fractional linear PDEs [8, 14, 17, 23] and Schrödinger-type equations [1, 3–6, 25].

For the second difficulty, the Laplace transform, usually used for the construction of ABCs, cannot be applied directly due to the nonlinear term. To handle the nonlinearity in the ABCs, a unified approach has been proposed in [57, 58] to construct accurate ABCs for the standard nonlinear Schrödinger equation ($\alpha = 1$). In this paper, we extend the unified approach to derive some nonlinear ABCs for the TFNSE involved in system (1.1). By using these ABCs, the original problem set in the unbounded domain is reduced to an initial boundary-value problem (IBVP), and *a priori* estimates for the reduced problem are stated. It is well-known that using an implicit numerical scheme for the nonlinear problem leads to an extra computational cost since the nonlinearity needs to be resolved through iterations, at each time step [2]. To avoid this problem, we construct a linearized finite-difference scheme by linearizing the nonlinear term. The convergence and stability analysis of the linearized scheme is established and the corresponding optimal convergence rate $\mathcal{O}(h^2 + \tau)$ is also obtained, where h and τ represent the spatial meshsize and time step, respectively.

The third difficulty concerns the huge storage and computational cost of the direct discretization of the Caputo derivative. For instances, the L1-approximation [32, 38, 40, 51] and high-order discretization schemes [15, 21, 37, 47] require the storage of all past values of the unknown function ψ , i.e. $\psi(0), \psi(\Delta t), \dots, \psi(n\Delta t)$, and $\mathcal{O}(n)$ flops at the n -th time step and each spatial grid point. Thus, the average storage is $\mathcal{O}(NJ)$ and the total computational cost is $\mathcal{O}(N^2J)$, where N and J are the total numbers of time steps and spatial grid points, respectively. As a consequence, this is a severe limitation for the long time simulations of time-fractional PDEs, that would be even worst for higher-dimensional problems. To reduce both the storage and computational cost, we use the fast evaluation of the Caputo derivative developed in [27]. The main idea of this method is to split the convolution integral in (1.2) into two parts: 1) a local part containing the integral from $t - \tau$ to t ($\tau > 0$), and 2) a history part for the integral from 0 to $t - \tau$. The standard L1-approximation is next used to discretize the local part. For the history part, we integrate by part to get a convolution integral of ψ with the kernel $t^{-1-\alpha}$. Thus, we can apply the sum-of-exponentials technique to approximate the kernel $t^{-1-\alpha}$ (with $0 < \alpha < 1$) on the interval $[\tau, T]$ with a uniform absolute error ε and for a number of exponentials $N_{\text{exp}} = \mathcal{O}\left(\log \frac{1}{\varepsilon} \left(\log \log \frac{1}{\varepsilon} + \log \frac{T}{\tau}\right) + \log \frac{1}{\tau} \left(\log \log \frac{1}{\varepsilon} + \log \frac{1}{\tau}\right)\right)$. For a fixed accuracy ε , we have $N_{\text{exp}} = \mathcal{O}(\log N)$ for $T \gg 1$ or $N_{\text{exp}} = \mathcal{O}(\log^2 N)$ for $T \approx 1$ assuming that $N = \frac{T}{\tau}$. The resulting algorithm has a nearly optimal complexity with $\mathcal{O}(N J N_{\text{exp}})$ operations and a $\mathcal{O}(J N_{\text{exp}})$ storage for solving the TFNSE. Indeed, the approximation can be used to accelerate the evaluation of

the convolution *via* the standard recurrence relation. Numerical examples show that the fast evaluation is both efficient and stable during the simulation.

The paper is organized as follows. In Section 2, we propose the construction of ABCs for the TFNSE based on the *unified approach*. In Section 3, we derive some *a priori* error estimates for the resulting truncated IBVP. Section 4 is devoted to the discretization scheme and its numerical analysis. Some numerical examples in Section 5 confirm the efficiency of the scheme and validate the error estimates. In addition, we provide some examples to illustrate the behavior of the solution of TFNSE. Finally, Section 6 concludes the paper.

2 Construction of nonlinear ABCs for the TFNSE

Let us introduce a computational bounded domain $\Omega^{\text{int}} := \{x_\ell < x < x_r\}$, with left and right finite fictitious boundaries $\Gamma^\ell := \{x_\ell\}$ and $\Gamma^r := \{x_r\}$. The two points x_ℓ and x_r are chosen such that the initial data $\psi_0(x)$ is compactly supported in Ω^{int} . We define the left and right half-spaces by $\Omega^\ell := \{-\infty < x < x_\ell\}$ and $\Omega^r := \{x_r < x < +\infty\}$, respectively, and the exterior domain by $\Omega^{\text{ext}} = \Omega^\ell \cup \Omega^r$. Let us apply now the basic ideas of the *unified approach* proposed in [57, 58] to construct some ABCs for the TFNSE

- (1) Firstly, the TFNSE arising in (1.1) is rewritten in operator form in the exterior domain Ω^{ext} as

$${}_i_0^C \mathcal{D}_t^\alpha \psi(x, t) = \mathcal{L}\psi(x, t) + \mathcal{N}\psi(x, t), \quad x \in \Omega^{\text{ext}}, \quad (2.1)$$

where the linear and nonlinear operators are respectively given by

$$\mathcal{L}\psi = -\psi_{xx} \quad \text{and} \quad \mathcal{N}\psi = V\psi + f(|\psi|^2)\psi.$$

Based on the operator splitting method [2, 11, 16], for a small time step, the original equation is considered as taking first a linear effect and next a nonlinear effect.

- (2) On Ω^{ext} , we approximate the linear operator \mathcal{L} by an approximate one-way operator \mathcal{L}^{app} (by distinguishing between the right- and left-traveling waves) which can absorb the wave striking the artificial boundaries. The one-directional operators \mathcal{L}^{app} are then used to replace the original linear operator \mathcal{L} .
- (3) Taking an infinitesimal time step, we obtain an approximate one-directional equation by coupling the approximate operator \mathcal{L}^{app} with the nonlinear operator \mathcal{N}

$${}_i_0^C \mathcal{D}_t^\alpha \psi(x, t) = \mathcal{L}^{\text{app}}\psi(x, t) + \mathcal{N}\psi(x, t). \quad (2.2)$$

Finally, applying the approximate equation (2.2) at the fictitious boundaries, one gets some ABCs. Therefore, the main point now is to construct the one-directional operators \mathcal{L}^{app} .

To derive an operator \mathcal{L}^{app} approximating \mathcal{L} , we first consider the following time-fractional linear Schrödinger equation (TFLSE) in the exterior domain

$${}_i_0^C \mathcal{D}_t^\alpha \psi(x, t) = \mathcal{L}\psi(x, t) = -\psi_{xx}(x, t), \quad x \in \Omega^{\text{ext}}, \quad (2.3)$$

$$\psi_0(x) = 0, \quad x \in \Omega^{\text{ext}}, \quad (2.4)$$

$$\psi(x, t) \rightarrow 0, \quad \text{when} \quad |x| \rightarrow +\infty. \quad (2.5)$$

Let us recall that the Laplace transform of the Caputo fractional derivative [59] is

$${}_0^C\mathcal{D}_t^\alpha[\widehat{\psi(t)}](s) = s^\alpha \widehat{\psi}(s) - s^{\alpha-1}\psi(0), \quad (2.6)$$

where the Laplace transform is defined by

$$\widehat{\psi}(s) = \int_0^{+\infty} e^{-st}\psi(t)dt, \quad \Re(s) > 0.$$

Thus Eq. (2.3) can be written in the Laplace domain as

$$is^\alpha \widehat{\psi}(x, s) = -\widehat{\psi}_{xx}(x, s), \quad \Re(s) > 0. \quad (2.7)$$

Setting $\sqrt{-i} = e^{-\frac{\pi i}{4}}$, the general form of the solution to Eq. (2.7) is

$$\widehat{\psi}(x, s) = A_-(s)e^{-\frac{\pi i}{4}}e^{-\sqrt{s^\alpha}x} + A_+(s)e^{-\frac{\pi i}{4}}e^{\sqrt{s^\alpha}x},$$

where the coefficients $A_\pm(s)$ are two arbitrary analytic functions. From (2.5), we deduce that

$$\widehat{\psi}(x, s) = \begin{cases} A_+(s)e^{-\frac{\pi i}{4}}e^{\sqrt{s^\alpha}x}, & x \in \Omega^\ell, \\ A_-(s)e^{-\frac{\pi i}{4}}e^{-\sqrt{s^\alpha}x}, & x \in \Omega^r. \end{cases} \quad (2.8)$$

Differentiating $\widehat{\psi}(x, s)$ with respect to x , one gets the two following relations

$$\partial_x \widehat{\psi}(x := x_\ell, s) = e^{-\frac{\pi i}{4}} s^{\frac{\alpha}{2}} \widehat{\psi}(x := x_\ell, s), \quad (2.9)$$

$$\partial_x \widehat{\psi}(x := x_r, s) = -e^{-\frac{\pi i}{4}} s^{\frac{\alpha}{2}} \widehat{\psi}(x := x_r, s), \quad (2.10)$$

which correspond to the Dirichlet-to-Neumann (DtN) maps at the interfaces for the TFLSE written in the Laplace domain.

Exact ABCs for the TFLSE. Applying the inverse Laplace transform to (2.9)-(2.10), one naturally gets the exact ABCs (DtN maps) for the TFLSE

$$\partial_{\mathbf{n}}\psi(x, t) = -\frac{e^{-\frac{\pi i}{4}}}{\Gamma(1 - \frac{\alpha}{2})} \int_0^t \frac{\partial_s \psi(x, s)}{(t-s)^{\frac{\alpha}{2}}} ds = -e^{-\frac{\pi i}{4}} {}_0^C\mathcal{D}_t^{\frac{\alpha}{2}} \psi(x, t), \quad \text{on } \Gamma^{\ell, r}. \quad (2.11)$$

In the above relation, we introduced $\partial_{\mathbf{n}}$ as the outwardly directed unit normal vector to $\Gamma^{\ell, r}$.

Approximate ABCs for the TFLSE. The exact ABCs (2.11) cannot be directly combined with the nonlinear term $\mathcal{N}\psi$. In addition, the above boundary condition is nonlocal and therefore computationally costly. To localize this boundary condition, we proceed as in the standard approach originally introduced by Engquist and Majda [20] for wave-like equations to obtain some local ABCs. To this aim, we first introduce the diagonal (P, P) -Padé approximation of the function $\sqrt{s^\alpha}$ used in [3–5, 9, 10, 28]

$$\sqrt{s^\alpha} = s_0^{\frac{\alpha}{2}} \left[1 - \sum_{p=1}^P \frac{A_p(s_0^\alpha - s^\alpha)}{s_0^\alpha - (s_0^\alpha - s^\alpha)B_p} \right] + E_P(s^\alpha), \quad (2.12)$$

where the coefficients $\{A_p\}_{1 \leq p \leq P}$ and $\{B_p\}_{1 \leq p \leq P}$ are given by

$$A_p = \frac{2}{2P+1} \sin^2 \left(\frac{p\pi}{2P+1} \right), \quad B_p = \cos^2 \left(\frac{p\pi}{2P+1} \right),$$

and the constant s_0 is the Padé expansion point. The error estimate of the Padé approximation is established in [43], for all $s^\alpha > 0$,

$$E_P(s^\alpha) = 2\sqrt{s^\alpha} \left(\frac{\gamma^{2P+1}(s^\alpha)}{1 + \gamma^{2P+1}(s^\alpha)} \right), \quad \text{with } \gamma(s^\alpha) = \frac{\sqrt{s^\alpha} - 1}{\sqrt{s^\alpha} + 1}. \quad (2.13)$$

Here, we only consider the simplest case, i.e. $P = 1$, and obtain the third-order diagonal Padé approximation

$$\sqrt{s^\alpha} \approx s_0^{\frac{\alpha}{2}} \frac{s_0^\alpha + 3s^\alpha}{3s_0^\alpha + s^\alpha}. \quad (2.14)$$

Replacing $\sqrt{s^\alpha}$ in (2.9) and (2.10) by the approximation (2.14), one gets

$$(3s_0^\alpha + s^\alpha) \partial_x \widehat{\psi}(x, s) \pm \mathbf{e}^{-\frac{\pi i}{4}} s_0^{\frac{\alpha}{2}} (s_0^\alpha + 3s^\alpha) \widehat{\psi}(x, s) = 0, \quad (2.15)$$

where the plus (minus, respectively) sign in \pm represents the right(left, respectively)-hand side boundary condition. After some simple algebraic calculations with (2.15), we deduce the relation

$$s^\alpha \widehat{\psi}(x, s) = -(\partial_x \pm 3\mathbf{e}^{-\frac{\pi i}{4}} s_0^{\frac{\alpha}{2}})^{-1} (3s_0^\alpha \partial_x \pm \mathbf{e}^{-\frac{\pi i}{4}} s_0^{\frac{\alpha}{2}} s_0^\alpha) \widehat{\psi}(x, s). \quad (2.16)$$

Applying the inverse Laplace transform to (2.16) and multiplying by i , one gets

$$i_0^C \mathcal{D}_t^\alpha \psi(x, t) = -i(\partial_x \pm 3\mathbf{e}^{-\frac{\pi i}{4}} s_0^{\frac{\alpha}{2}})^{-1} (3s_0^\alpha \partial_x \pm \mathbf{e}^{-\frac{\pi i}{4}} s_0^{\frac{\alpha}{2}} s_0^\alpha) \psi(x, t). \quad (2.17)$$

Comparing (2.17) with (2.3), we can derive the approximate operator

$$\mathcal{L}^{\text{app}} = -i(\partial_x \pm 3\mathbf{e}^{-\frac{\pi i}{4}} s_0^{\frac{\alpha}{2}})^{-1} (3s_0^\alpha \partial_x \pm \mathbf{e}^{-\frac{\pi i}{4}} s_0^{\frac{\alpha}{2}} s_0^\alpha) \psi(x, t). \quad (2.18)$$

Nonlinear approximate ABCs for the TFNSE. Substituting (2.18) into (2.2), the nonlinear ABCs for the TFNSE are

$$(\partial_x \pm 3\mathbf{e}^{-\frac{\pi i}{4}} s_0^{\frac{\alpha}{2}})_0^C \mathcal{D}_t^\alpha \psi + (3s_0^\alpha \partial_x \pm \mathbf{e}^{-\frac{\pi i}{4}} s_0^{\frac{\alpha}{2}} s_0^\alpha) \psi = -i(\partial_x \pm 3\mathbf{e}^{-\frac{\pi i}{4}} s_0^{\frac{\alpha}{2}}) (V\psi + f(|\psi|^2)\psi). \quad (2.19)$$

By using an approach similar to the one by Kuska [30], we linearize the nonlinear term $f(|\psi|^2)$ to obtain a variety of boundary conditions:

$$(\partial_x \pm 3\mathbf{e}^{-\frac{\pi i}{4}} s_0^{\frac{\alpha}{2}})_0^C \mathcal{D}_t^\alpha \psi + (3s_0^\alpha \partial_x \pm \mathbf{e}^{-\frac{\pi i}{4}} s_0^{\frac{\alpha}{2}} s_0^\alpha) \psi = -i(V + f(|\psi|^2))(\partial_x \psi \pm 3\mathbf{e}^{-\frac{\pi i}{4}} s_0^{\frac{\alpha}{2}} \psi). \quad (2.20)$$

Finally, we obtain an IBVP in $\Omega^{\text{int}} \times [0, T]$ with the boundary conditions (2.20) on $\Gamma^{\ell, r}$

$$i_0^C \mathcal{D}_t^\alpha \psi(x, t) = -\psi_{xx} + V\psi + f(|\psi|^2)\psi, \quad t > 0, x \in \Omega^{\text{int}}, \quad (2.21)$$

$$\psi(x, 0) = \psi_0(x), \quad x \in \Omega^{\text{int}}, \quad (2.22)$$

$$(\partial_x \mp 3\mathbf{e}^{-\frac{\pi i}{4}} s_0^{\frac{\alpha}{2}})_0^C \mathcal{D}_t^\alpha \psi + (3s_0^\alpha \partial_x \mp \mathbf{e}^{-\frac{\pi i}{4}} s_0^{\frac{\alpha}{2}} s_0^\alpha) \psi = -i(V + f(|\psi|^2))(\partial_x \mp 3\mathbf{e}^{-\frac{\pi i}{4}} s_0^{\frac{\alpha}{2}}) \psi, \quad x \in \Gamma^{\ell, r}. \quad (2.23)$$

Remark 1 Generally, the ABCs (2.19) perform better than (2.20). However, the stability analysis with (2.20) is easier to handle than with (2.19). The comparison is discussed in [60] for general nonlinear Schrödinger equations. In this paper, we consider (2.20) as ABC.

3 *A priori* error estimates

To state the stability of (2.21)-(2.23), we introduce two auxiliary variables

$$\begin{aligned}\theta(t) &= \partial_x \psi(x_\ell, t) - 3s_0^{\frac{\alpha}{2}} e^{-\frac{\pi i}{4}} \psi(x_\ell, t), \\ \phi(t) &= \partial_x \psi(x_r, t) + 3s_0^{\frac{\alpha}{2}} e^{-\frac{\pi i}{4}} \psi(x_r, t).\end{aligned}$$

Thus, the reduced problem (2.21)-(2.23) can be equivalently rewritten as

$$i_0^C \mathcal{D}_t^\alpha \psi(x, t) = -\psi_{xx} + V\psi + f(|\psi|^2)\psi, \quad x \in \Omega^{\text{int}}, \quad t > 0, \quad (3.1)$$

$$\psi(x, 0) = \psi_0(x), \quad x \in \Omega^{\text{int}}, \quad (3.2)$$

$$\psi_x(x, t) = \theta(t) + 3s_0^{\frac{\alpha}{2}} e^{-\frac{\pi i}{4}} \psi(x, t), \quad x \in \Gamma^\ell, \quad (3.3)$$

$${}_0^C \mathcal{D}_t^\alpha \theta(t) + i(V(x) + f(|\psi|^2))\theta(t) + 3s_0^\alpha \theta(t) + 8s_0^{\frac{3\alpha}{2}} e^{-\frac{\pi i}{4}} \psi(x, t) = 0, \quad x \in \Gamma^\ell, \quad (3.4)$$

$$\psi_x(x, t) = \phi(t) - 3s_0^{\frac{\alpha}{2}} e^{-\frac{\pi i}{4}} \psi(x, t), \quad x \in \Gamma^r, \quad (3.5)$$

$${}_0^C \mathcal{D}_t^\alpha \phi(t) + i(V + f(|\psi|^2))\phi(t) + 3s_0^\alpha \phi(t) - 8s_0^{\frac{3\alpha}{2}} e^{-\frac{\pi i}{4}} \psi(x, t) = 0, \quad x \in \Gamma^r. \quad (3.6)$$

Some useful lemmas are now given to state some *a priori* estimates for the reduced problem (3.1)-(3.6).

Lemma 3.1 *Let $u(t)$ be a complex-valued function which is absolutely continuous on $[0, T]$. Then, the following inequality holds*

$${}_0^C \mathcal{D}_t^\alpha |u(t)|^2 \leq \bar{u}(t) {}_0^C \mathcal{D}_t^\alpha u(t) + u(t) {}_0^C \mathcal{D}_t^\alpha \bar{u}(t), \quad 0 < \alpha < 1, \quad (3.7)$$

where $|u|^2 = \bar{u}u$ and \bar{u} represents the complex conjugate function of u .

Proof. A direct calculation (considering the order of integration) is given as follows

$$\begin{aligned}& \bar{u}(t) {}_0^C \mathcal{D}_t^\alpha u(t) + u(t) {}_0^C \mathcal{D}_t^\alpha \bar{u}(t) - {}_0^C \mathcal{D}_t^\alpha |u(t)|^2 \\ &= \frac{1}{\Gamma(1-\alpha)} \left[\int_0^t \frac{u_\tau(\tau) \bar{u}(t)}{(t-\tau)^\alpha} d\tau + \int_0^t \frac{u(t) \bar{u}_\tau(\tau)}{(t-\tau)^\alpha} d\tau - \int_0^t \frac{u(\tau) \bar{u}_\tau(\tau) + \bar{u}(\tau) u_\tau(\tau)}{(t-\tau)^\alpha} d\tau \right] \\ &= \frac{1}{\Gamma(1-\alpha)} \left[\int_0^t \frac{u_\tau(\tau) [\bar{u}(t) - \bar{u}(\tau)]}{(t-\tau)^\alpha} d\tau + \int_0^t \frac{\bar{u}_\tau(\tau) [u(t) - u(\tau)]}{(t-\tau)^\alpha} d\tau \right] \\ &= \frac{1}{\Gamma(1-\alpha)} \left[\int_0^t \frac{u_\tau(\tau)}{(t-\tau)^\alpha} \int_\tau^t \bar{u}_\eta(\eta) d\eta d\tau + \int_0^t \frac{\bar{u}_\tau(\tau)}{(t-\tau)^\alpha} \int_\tau^t u_\eta(\eta) d\eta d\tau \right] \\ &= \frac{1}{\Gamma(1-\alpha)} \left[\int_0^t \bar{u}_\eta(\eta) d\eta \int_0^\eta \frac{u_\tau(\tau)}{(t-\tau)^\alpha} d\tau + \int_0^t u_\eta(\eta) d\eta \int_0^\eta \frac{\bar{u}_\tau(\tau)}{(t-\tau)^\alpha} d\tau \right] \\ &= \frac{1}{\Gamma(1-\alpha)} \left[\int_0^t \frac{(t-\eta)^\alpha \bar{u}_\eta(\eta)}{(t-\eta)^\alpha} d\eta \int_0^\eta \frac{u_\tau(\tau)}{(t-\tau)^\alpha} d\tau + \int_0^t \frac{(t-\eta)^\alpha u_\eta(\eta)}{(t-\eta)^\alpha} d\eta \int_0^\eta \frac{\bar{u}_\tau(\tau)}{(t-\tau)^\alpha} d\tau \right] \\ &= \frac{1}{\Gamma(1-\alpha)} \int_0^t (t-\eta)^\alpha \frac{\partial}{\partial \eta} \left| \int_0^\eta \frac{u_\tau(\tau)}{(t-\tau)^\alpha} d\tau \right|^2 d\eta \\ &= \frac{\alpha}{\Gamma(1-\alpha)} \int_0^t (t-\eta)^{1-\alpha} \left| \int_0^\eta \frac{u_\tau(\tau)}{(t-\tau)^\alpha} d\tau \right|^2 d\eta \geq 0.\end{aligned}$$

■

Now, let us consider the following Lemma (see e.g. [49]).

Lemma 3.2 Let $0 < \alpha < 1$. We assume that $y(t)$ is a nonnegative absolutely continuous function that satisfies

$${}_0^C \mathcal{D}_t^\alpha y(t) \leq c_1 y(t) + c_2(t), \quad 0 < \alpha < 1, \quad t \in (0, T], \quad (3.8)$$

where $c_1 > 0$ and $c_2(t)$ is an integrable nonnegative function on $[0, T]$. Then, we have

$$y(t) \leq y(0)E_{\alpha,1}(c_1 t^\alpha) + \Gamma(\alpha)E_{\alpha,\alpha}(c_1 t^\alpha) {}_0 \mathcal{D}_t^{-\alpha} c_2(t), \quad (3.9)$$

where $E_{\alpha,\beta}(z) = \sum_{n=0}^{\infty} \frac{z^n}{\Gamma(n\alpha + \beta)}$ are the Mittag-Leffler functions and $\mathcal{D}_t^{-\alpha} u(t)$ is the Riemann-Liouville integral given by

$${}_0 \mathcal{D}_t^{-\alpha} u(t) = \frac{1}{\Gamma(\alpha)} \int_0^t \frac{u(\tau)}{(t-\tau)^{1-\alpha}} d\tau, \quad 0 < \alpha < 1.$$

We can then deduce the following result.

Theorem 3.3 Let $(\psi(x, t), \phi(t), \theta(t))$ be the solution of the reduced problem (3.1)-(3.6). Then, for $0 < \alpha < 1$, we have the following a priori estimate

$$\int_{x_\ell}^{x_r} |\psi(x, t)|^2 dx + \frac{1}{8} s_0^{-\frac{3\alpha}{2}} (|\phi(t)|^2 + |\theta(t)|^2) \leq \int_{x_\ell}^{x_r} |\psi_0(x)|^2 dx. \quad (3.10)$$

Proof. By multiplying (3.1) by $\bar{\psi}(x, t)$, integrating by parts the result over Ω^{int} , taking the complex conjugate of (3.1), multiplying the result by $\psi(x, t)$ and integrating by parts over Ω^{int} , and finally combining the two equations and taking the complex parts, we have

$$\int_{x_\ell}^{x_r} [\bar{\psi}(x, t) {}_0^C \mathcal{D}_t^\alpha \psi(x, t) + \psi(x, t) {}_0^C \mathcal{D}_t^\alpha \bar{\psi}(x, t)] dx = 2\Im \{ \bar{\psi} \psi_x \} \Big|_{x_\ell}^{x_r}. \quad (3.11)$$

Substituting $\psi_x(x_\ell, t)$ and $\psi_x(x_r, t)$, defined by (3.3) and (3.5), into (3.11), we arrive at

$$\begin{aligned} & \int_{x_\ell}^{x_r} [\bar{\psi}(x, t) {}_0^C \mathcal{D}_t^\alpha \psi(x, t) + \psi(x, t) {}_0^C \mathcal{D}_t^\alpha \bar{\psi}(x, t)] dx \\ &= -3\sqrt{2} s_0^{\frac{\alpha}{2}} (|\psi(x_\ell, t)|^2 + |\psi(x_r, t)|^2) + 2\Im \left\{ e^{-\frac{\pi i}{4}} (\phi(t) \bar{\psi}(x_r, t) - \theta \bar{\psi}(x_\ell, t)) \right\}. \end{aligned} \quad (3.12)$$

Multiplying (3.6) by $\frac{1}{8} s_0^{-\frac{3\alpha}{2}} \bar{\phi}(x_r, t)$, then taking the complex conjugate of (3.6), multiplying the result by $\frac{1}{8} s_0^{-\frac{3\alpha}{2}} \phi(x_r, t)$, combining the two equations, taking the real parts, and using the same arguments as (3.4), we obtain

$$\frac{1}{8} s_0^{-\frac{3\alpha}{2}} [\bar{\theta}(t) {}_0^C \mathcal{D}_t^\alpha \theta(t) + \theta(t) {}_0^C \mathcal{D}_t^\alpha \bar{\theta}(t)] = -\frac{3}{4} s_0^{-\frac{\alpha}{2}} |\theta(t)|^2 - 2\Re \{ e^{-\frac{\pi i}{4}} \theta(t) \bar{\psi}(x_\ell, t) \}, \quad (3.13)$$

$$\frac{1}{8} s_0^{-\frac{3\alpha}{2}} [\bar{\phi}(t) {}_0^C \mathcal{D}_t^\alpha \phi(t) + \phi(t) {}_0^C \mathcal{D}_t^\alpha \bar{\phi}(t)] = -\frac{3}{4} s_0^{-\frac{\alpha}{2}} |\phi(t)|^2 + 2\Re \{ e^{-\frac{\pi i}{4}} \phi(t) \bar{\psi}(x_r, t) \}. \quad (3.14)$$

Adding (3.12), (3.13) and (3.14), applying Lemma 3.1 and noticing that $|\Im\{Z\}| + |\Re\{Z\}| \leq \sqrt{2}|Z|$ lead to

$$\begin{aligned} & {}_0^C \mathcal{D}_t^\alpha \int_{x_\ell}^{x_r} |\psi(x, t)|^2 dx + \frac{1}{8} s_0^{-\frac{3\alpha}{2}} {}_0^C \mathcal{D}_t^\alpha [|\phi(t)|^2 + |\theta(t)|^2] \\ & \leq -3\sqrt{2} s_0^{\frac{\alpha}{2}} (|\psi(x_\ell, t)|^2 + |\psi(x_r, t)|^2) + \frac{3}{8} s_0^{-\frac{\alpha}{2}} (|\theta(t)|^2 + |\phi(t)|^2) + 2\sqrt{2} (|\phi(t) \bar{\psi}| + |\theta \bar{\psi}|). \end{aligned} \quad (3.15)$$

Applying the Cauchy-Schwarz inequality

$$|\theta(t)\bar{\psi}(x_\ell, t)| \leq \frac{1}{4\epsilon}|\theta(t)|^2 + \epsilon|\psi(x_\ell, t)|^2 \quad \text{and} \quad |\phi(t)\bar{\psi}(x_r, t)| \leq \frac{1}{4\epsilon}|\phi(t)|^2 + \epsilon|\psi(x_r, t)|^2,$$

with $\epsilon = \frac{3}{2}s_0^{\frac{\alpha}{2}}$ to Eq. (3.15), we get

$${}^C_0\mathcal{D}_t^\alpha \left[\int_{x_\ell}^{l^+} |\psi(x, t)|^2 dx + \frac{1}{8}s_0^{-\frac{3\alpha}{2}} (|\phi(t)|^2 + |\theta(t)|^2) \right] \leq -\frac{9}{24}s_0^{-\frac{\alpha}{2}} (|\phi(t)|^2 + |\theta(t)|^2) \leq 0. \quad (3.16)$$

Finally applying Lemma (3.2) completes the proof. \blacksquare

4 Discretization and analysis of the schemes

This section is devoted to the construction and numerical analysis of the linearized numerical schemes. Let $\tau = T/N$ and $h = (x_\ell - x_r)/J$ be the temporal and spatial step sizes, respectively, where N and J are two given positive integers. We denote the discrete time by $t_n = n\tau$ ($0 \leq n \leq N$) and $\Omega_\tau = \{t_n | 0 = t_0 < t_1 < \dots < t_N = T\}$. A point of the uniform spatial grid is such that $x_j = jh$, ($0 \leq j \leq J$), and $\Omega_h = \{x_j | x_j = x_\ell + jh, 0 \leq j \leq J\}$. We also set

$$\psi_j^n = \psi(x_j, t_n), \quad V_j = V(x_j), \quad \phi^n = \phi(t_n), \quad \theta^n = \theta(t_n).$$

4.1 Derivation of the linearized L1-scheme

The L1-scheme for approximating the Caputo fractional derivative is

$$\begin{aligned} {}^C_0\mathcal{D}_{t_n}^\alpha v &= \frac{1}{\Gamma(1-\alpha)} \int_0^{t_n} \frac{v'(s)}{(t_n-s)^\alpha} ds = \frac{1}{\Gamma(1-\alpha)} \sum_{k=1}^n \frac{v^k - v^{k-1}}{\tau} \int_{t_{k-1}}^{t_k} \frac{1}{(t_n-s)^\alpha} ds + Q^n \\ &= \frac{\tau^{-\alpha}}{\Gamma(2-\alpha)} \sum_{k=1}^n a_{n-k} (v^k - v^{k-1}) + Q^n, \end{aligned}$$

where $v^n = v(t_n)$ and $a_k = (k+1)^{1-\alpha} - k^{1-\alpha}$, $k \geq 0$. Let us denote the L1 scheme by

$${}^C_0\mathbb{D}_\tau^\alpha = \frac{\tau^{-\alpha}}{\Gamma(2-\alpha)} \sum_{k=1}^n a_{n-k} (v^k - v^{k-1}).$$

If $v \in C^2([0, T])$, the truncation error Q^n satisfies [40, 51]

$$|Q^n| \leq C\tau^{2-\alpha}. \quad (4.1)$$

For a sequence of functions $\{w_j^n\}_{0 \leq n \leq N, 0 \leq j \leq J}$, we define

$$\begin{aligned} \delta_x w_{j+\frac{1}{2}}^n &= \frac{w_{j+1}^n - w_j^n}{h}, & \delta_x^2 w_j^n &= \frac{1}{h} (\delta_x w_{j+\frac{1}{2}}^n - \delta_x w_{j-\frac{1}{2}}^n), \\ \delta_t w_j^n &= \frac{w_j^n - w_j^{n-1}}{\tau}, & D_\tau^\alpha w_j^n &:= \frac{\tau^{-\alpha}}{\Gamma(2-\alpha)} \sum_{i=1}^n a_{n-i} \delta_t w_j^i. \end{aligned} \quad (4.2)$$

Writing the TFNSE equation at the left point x_ℓ

$$i {}_0^C \mathcal{D}_t^\alpha \psi_0^n = -(\psi_0^n)_{xx} + V_0 \psi_0^n + f(|\psi_0^n|^2) \psi_0^n,$$

and using the Taylor expansion, we have

$$\begin{aligned} (\psi_0^n)_x &= \frac{1}{h}(\psi_1^n - \psi_0^n) - \frac{h}{2}(\psi_0^n)_{xx} + \mathcal{O}(h^2) \\ &= \delta_x \psi_{\frac{1}{2}}^n + \frac{h}{2} \left(i {}_0^C \mathcal{D}_t^\alpha \psi_0^n - (V_0 + f(|\psi_0^n|^2)) \psi_0^n \right) + \mathcal{O}(h^2). \end{aligned} \quad (4.3)$$

Similarly, at the right boundary point x_J , we have

$$(\psi_J^n)_x = \delta_x \psi_{J-\frac{1}{2}}^n - \frac{h}{2} \left(i {}_0^C \mathcal{D}_t^\alpha \psi_J^n - (V_J + f(|\psi_J^n|^2)) \psi_J^n \right) + \mathcal{O}(h^2). \quad (4.4)$$

We apply the L1-scheme to approximate the time-fractional Caputo derivative, the second-order central finite difference method to approximate the second-order spatial derivative at the interior points, and use (4.3) and (4.4) to couple the ABCs and the linearized approach to deal with the nonlinear term. This yields

$$i {}_0^C \mathcal{D}_\tau^\alpha \psi_j^n = -\delta_x^2 \psi_j^n + [V_j + f(|\psi_j^{n-1}|^2)] \psi_j^n + T_j^n, \quad 1 \leq j \leq J-1, 1 \leq n \leq N, \quad (4.5)$$

$$i \frac{h}{2} {}_0^C \mathcal{D}_\tau^\alpha \psi_0^n = -\delta_x \psi_{\frac{1}{2}}^n + (\theta^n + 3s_0^{\frac{\alpha}{2}} e^{-\frac{\pi i}{4}} \psi_0^n) + \frac{h}{2} [V_0 + f(|\psi_0^{n-1}|^2)] \psi_0^n + T_0^n, \quad (4.6)$$

$${}_0^C \mathcal{D}_\tau^\alpha \theta^n = -i [V_0 + f(|\psi_0^{n-1}|^2)] \theta^n - 3s_0^\alpha \theta^n - 8s_0^{\frac{3\alpha}{2}} e^{-\frac{\pi i}{4}} \psi_0^n + R_0^n, \quad (4.7)$$

$$i \frac{h}{2} {}_0^C \mathcal{D}_\tau^\alpha \psi_J^n = \delta_x \psi_{J-\frac{1}{2}}^n + (3s_0^{\frac{\alpha}{2}} e^{-\frac{\pi i}{4}} \psi_J^n - \phi^n) + \frac{h}{2} [V_J + f(|\psi_J^{n-1}|^2)] \psi_J^n + T_J^n, \quad (4.8)$$

$${}_0^C \mathcal{D}_\tau^\alpha \phi^n = -i [V_J + f(|\psi_J^{n-1}|^2)] \phi^n - 3s_0^\alpha \phi^n + 8s_0^{\frac{3\alpha}{2}} e^{-\frac{\pi i}{4}} \psi_J^n + R_J^n, \quad (4.9)$$

$$\psi_j^0 = \psi_0(x_j), \quad 0 \leq j \leq J. \quad (4.10)$$

Applying the Taylor expansion and (4.1), we have

$$|T_j^n| \leq C(\tau + h^2), \quad 1 \leq j \leq J-1, \quad 1 \leq n \leq N, \quad (4.11)$$

$$|T_0^n| \leq C(\tau + h^2), \quad |T_J^n| \leq C(\tau + h^2), \quad 1 \leq n \leq N, \quad (4.12)$$

$$|R_0^n| \leq C\tau, \quad |R_J^n| \leq C\tau, \quad 1 \leq n \leq N. \quad (4.13)$$

Omitting the small terms in (4.5)-(4.10) based on the above error bounds, we construct the following finite difference scheme for solving problem (3.1)-(3.4)

$$i \mathcal{D}_\tau^\alpha \Psi_j^n = -\delta_x^2 \Psi_j^n + [V_j + f(|\Psi_j^{n-1}|^2)] \Psi_j^n, \quad 1 \leq j \leq J-1, 1 \leq n \leq N, \quad (4.14)$$

$$i \frac{h}{2} \mathcal{D}_\tau^\alpha \Psi_0^n = -\delta_x \Psi_{\frac{1}{2}}^n + (\Theta^n + 3s_0^{\frac{\alpha}{2}} e^{-\frac{\pi i}{4}} \Psi_0^n) + \frac{h}{2} [V_0 + f(|\Psi_0^{n-1}|^2)] \Psi_0^n, \quad (4.15)$$

$$\mathcal{D}_\tau^\alpha \Theta^n = -i [V_0 + f(|\Psi_0^{n-1}|^2)] \Theta^n - 3s_0^\alpha \Theta^n - 8s_0^{\frac{3\alpha}{2}} e^{-\frac{\pi i}{4}} \Psi_0^n, \quad (4.16)$$

$$i \frac{h}{2} \mathcal{D}_\tau^\alpha \Psi_J^n = \delta_x \Psi_{J-\frac{1}{2}}^n + (3s_0^{\frac{\alpha}{2}} e^{-\frac{\pi i}{4}} \Psi_J^n - \Phi^n) + \frac{h}{2} [V_J + f(|\Psi_J^{n-1}|^2)] \Psi_J^n, \quad (4.17)$$

$$\mathcal{D}_\tau^\alpha \Phi^n = -i [V_J + f(|\Psi_J^{n-1}|^2)] \Phi^n - 3s_0^\alpha \Phi^n + 8s_0^{\frac{3\alpha}{2}} e^{-\frac{\pi i}{4}} \Psi_J^n, \quad (4.18)$$

$$\Psi_j^0 = \Psi_0(x_j), \quad 0 \leq j \leq J, \quad (4.19)$$

where Ψ_j^n , Φ^n and Θ^n correspond to the numerical approximations of ψ_j^n , ϕ^n and θ^n , respectively.

4.2 Numerical analysis of the linearized L1-scheme

Let us now consider the convergence analysis of the finite difference scheme. Let $u = \{(u_0, u_1, \dots, u_J)\}$ and $v = \{(v_0, v_1, \dots, v_J)\}$ defined on Ω_h . We introduce the following inner products and norms

$$(u, v) = h\left(\frac{1}{2}\bar{u}_0v_0 + \sum_{j=1}^{J-1}\bar{u}_jv_j + \frac{1}{2}\bar{u}_Jv_J\right), \quad \|u\| = \sqrt{(u, u)},$$

$$|u|_1 = \sqrt{h \sum_{j=1}^J |\delta_x \bar{u}_{j-\frac{1}{2}}| |\delta_x u_{j-\frac{1}{2}}|}, \quad \|u\|_\infty = \max_{0 \leq j \leq J} |u_j|.$$

We first introduce the following set of useful lemmas.

Lemma 4.1 (see [51]) *We assume that $a_k = (k+1)^{1-\alpha} - k^{1-\alpha}$. Then, one gets*

$$1 = a_0 > a_1 > \dots > a_n \rightarrow 0. \quad (4.20)$$

Lemma 4.2 *For any discrete function $v \in \Omega_h$, the following inequality holds*

$$\|v\|_\infty^2 \leq \epsilon |v|_1^2 + \left(\frac{1}{\epsilon} + \frac{1}{x_r - x_\ell}\right) \|v\|^2.$$

Lemma 4.3 (see [39]) *Suppose that $\{\omega^n\}_{n=0, \dots}$ and $\{g^n\}_{n=0, \dots}$ are two nonnegative sequences that satisfy $\omega^0 \leq g^0$ and*

$$D_\tau^\alpha \omega^n \leq \lambda_1 \omega^n + \lambda_2 \omega^{n-1} + g^n, \quad n \geq 1,$$

where $\lambda_1 > 0$ and $\lambda_2 \geq 0$ are two given real-valued constants. Then, there exists a constant τ^* such that, for $\tau \leq \tau^*$,

$$\omega^n \leq 2\left(\omega^0 + \frac{t_n^\alpha}{\Gamma(1+\alpha)} \max_{0 \leq j \leq n} g^j\right) E_\alpha(2\lambda t_n) \quad 1 \leq n \leq N, \quad (4.21)$$

where $E_\alpha(z) = E_{\alpha,1}(z)$ and $\lambda = \lambda_1 + \frac{\lambda_2}{2-2\alpha}$.

Lemma 4.4 *Let $\{v^n\}_{n=0}^N$ be a sequence of functions defined in Ω_τ . If $v_0 \leq \kappa$ and*

$$\Re(D_\tau^\alpha v^n, v^n) \leq C \|v^{n-1}\|^2 + C \|v^n\|^2 + \kappa^2, \quad 1 \leq n \leq N, \quad (4.22)$$

where $\kappa > 0$ and C is a positive constant bounded independently of τ , then, there exists a positive constant τ_* such that, for $\tau < \tau_*$,

$$\|v^n\| \leq C\kappa. \quad (4.23)$$

Proof. From the definition of D_τ^α and Lemma 3.1, we have

$$\begin{aligned} \Re({}_0^C D_\tau^\alpha v^n, v^n) &= \Re\left(\frac{\tau^{2-\alpha}}{\Gamma(2-\alpha)} \left(a_0 v^n - \sum_{j=1}^{n-1} (a_{n-j-1} - a_{n-j}) v^j - a_{n-1} v^0, v^n\right)\right) \\ &\geq \frac{\tau^{2-\alpha}}{\Gamma(2-\alpha)} \left(a_0 \|v^n\|^2 - \sum_{j=1}^{n-1} (a_{n-j-1} - a_{n-j}) \frac{\|v^j\|^2 + \|v^n\|^2}{2} - a_{n-1} \frac{\|v^0\|^2 + \|v^n\|^2}{2}\right) \\ &= \frac{\tau^{2-\alpha}}{2\Gamma(2-\alpha)} \left(a_0 \|v^n\|^2 - \sum_{j=1}^{n-1} (a_{n-j-1} - a_{n-j}) \|v^j\|^2 - a_{n-1} \|v^0\|^2\right) \\ &= \frac{1}{2} D_\tau^\alpha \|v^n\|^2. \end{aligned} \quad (4.24)$$

Substituting (4.24) into (4.22) and using Lemma 4.3, we can easily get (4.23). \blacksquare

We now define the error function on the grid, for $0 \leq j \leq J$, $0 \leq n \leq N$,

$$e_j^n = \psi_j^n - \Psi_j^n, \quad \varphi^n = \phi^n - \Phi^n, \quad \vartheta = \theta^n - \Theta^n,$$

and let $K = \max_{1 \leq n \leq N} \{\|\psi^n\|_\infty + |\phi^n| + |\theta^n|\} + 1$.

We have the following result.

Theorem 4.5 *Let us assume that system (3.1)-(3.4) has unique smooth solutions $\psi(x, t)$, $\theta(t)$ and $\phi(t)$ in $\Omega^{int} \times [0, T]$. Then, there exist two positive constants τ_0 and h_0 such that, when $\tau \leq \tau_0$ and $h \leq h_0$, system (4.14)-(4.19) admits a unique solution $\{\Psi_j^n, \Phi^n, \Theta^n\}$, for $n = 1, 2, \dots, N$, satisfying*

$$\|\Psi^n\|_\infty + |\Theta^n| + |\Phi^n| \leq K, \quad (4.25)$$

$$\|e^n\| + |\varphi^n| + |\vartheta^n| \leq C^*(\tau + h^2). \quad (4.26)$$

Proof. At each discrete time $t = t_n$, the proposed numerical method produces a tridiagonal system of linear algebraic equations. Since the associated matrix is strictly diagonally dominant, then the numerical solution of the problem is unique.

Now, we prove the error estimates of the numerical scheme. Subtracting (4.14)-(4.19) from (4.5)-(4.10), we have the error equations: for $1 \leq n \leq N$

$$i {}_0^C \mathbb{D}_\tau^\alpha e_j^n = -\delta_x^2 e_j^n + V_j e_j^n + f(|\psi_j^{n-1}|^2) \psi_j^n - f(|\Psi_j^{n-1}|^2) \Psi_j^n + T_j^n, \quad 1 \leq j \leq J-1, \quad (4.27)$$

$$i \frac{h}{2} {}_0^C \mathbb{D}_\tau^\alpha e_0^n = -\delta_x e_{\frac{1}{2}}^n + (\vartheta^n + 3s_0^{\frac{\alpha}{2}} e^{-\frac{\pi i}{4}} e_0^n) + \frac{h}{2} V_0 e_0^n + \frac{h}{2} \left(f(|\psi_0^{n-1}|^2) \psi_0^n - f(|\Psi_0^{n-1}|^2) \Psi_0^n \right) + T_0^n, \quad (4.28)$$

$${}_0^C \mathbb{D}_\tau^\alpha \vartheta^n = -i \left(V_0 \vartheta^n + f(|\psi_0^{n-1}|^2) \theta^n - f(|\Psi_0^{n-1}|^2) \Theta^n \right) - 3s_0^\alpha \vartheta^n - 8s_0^{3\alpha/2} e^{-\frac{\pi i}{4}} e_0^n + R_0^n, \quad (4.29)$$

$$i \frac{h}{2} {}_0^C \mathbb{D}_\tau^\alpha e_J^n = \delta_x e_{J-\frac{1}{2}}^n + (3s_0^{\frac{\alpha}{2}} e^{-\frac{\pi i}{4}} e_J^n - \varphi^n) + \frac{h}{2} V_J e_J^n + \frac{h}{2} \left(f(|\psi_J^{n-1}|^2) \psi_J^n - f(|\Psi_J^{n-1}|^2) \Psi_J^n \right) + T_J^n, \quad (4.30)$$

$${}_0^C \mathbb{D}_\tau^\alpha \varphi^n = -i \left[V_J \varphi^n + f(|\psi_J^{n-1}|^2) \phi^n - f(|\Psi_J^{n-1}|^2) \Phi^n \right] - 3s_0^\alpha \varphi^n + 8s_0^{\frac{3\alpha}{2}} e^{-\frac{\pi i}{4}} e_J^n + R_J^n, \quad (4.31)$$

$$e_j^0 = 0, \quad 0 \leq j \leq J. \quad (4.32)$$

Multiplying Eq. (4.27) by $h \bar{e}_j^n$, and summing up over j from 1 to $J-1$, we have

$$ih \sum_{j=1}^{J-1} ({}_0^C \mathbb{D}_\tau^\alpha e_j^n) \bar{e}_j^n = h \sum_{j=1}^{J-1} \left\{ -(\delta_x^2 e_j^n) \bar{e}_j^n + V_j e_j^n \bar{e}_j^n + \left[f(|\psi_j^{n-1}|^2) \psi_j^n - f(|\Psi_j^{n-1}|^2) \Psi_j^n \right] \bar{e}_j^n + T_j^n \bar{e}_j^n \right\}.$$

Multiplying \bar{e}_0^n , $i \bar{\vartheta}^n$, \bar{e}_J^n and $i \bar{\varphi}^n$ on both sides of (4.28)-(4.31), respectively, adding the results with the above formula, then using the following summation by parts formulas

$$-h \sum_{j=1}^{J-1} (\delta_x^2 e_j^n) \bar{e}_j^n - \bar{e}_0^n \delta_x e_{\frac{1}{2}}^n + \bar{e}_J^n \delta_x e_{J-\frac{1}{2}}^n = |e^n|_1^2$$

and

$$h \left(\frac{1}{2} \bar{e}_0^n {}_0^C \mathbb{D}_\tau^\alpha e_0^n + \sum_{j=1}^{J-1} ({}_0^C \mathbb{D}_\tau^\alpha e_j^n) \bar{e}_j^n + \frac{1}{2} \bar{e}_J^n {}_0^C \mathbb{D}_\tau^\alpha e_J^n \right) = \left({}_0^C \mathbb{D}_\tau^\alpha e^n, e^n \right),$$

we arrive at

$$\begin{aligned}
& i \left({}_0^C \mathbb{D}_\tau^\alpha e^n, e^n \right) + i \bar{\varphi}^n {}_0^C \mathbb{D}_\tau^\alpha \varphi^n + i \bar{\vartheta}^n {}_0^C \mathbb{D}_\tau^\alpha \vartheta^n \\
&= |e^n|_1^2 + h \sum_{j=1}^{J-1} V_j e_j^n \bar{e}_j^n + h \sum_{j=1}^{J-1} \left[f(|\psi_j^{n-1}|^2) \psi_j^n - f(|\Psi_j^{n-1}|^2) \Psi_j^n \right] \bar{e}_j^n + h \sum_{j=1}^{J-1} T_j^n \bar{e}_j^n \\
&+ (\vartheta^n + 3s_0^{\frac{\alpha}{2}} \mathbf{e}^{-\frac{\pi}{4}i} e_0^n) \bar{e}_0^n + \frac{h}{2} V_0 e_0^n \bar{e}_0^n + \frac{h}{2} \left(f(|\psi_0^{n-1}|^2) \psi_0^n - f(|\Psi_0^{n-1}|^2) \Psi_0^n \right) \bar{e}_0^n + T_0^n \bar{e}_0^n \\
&+ \left(V_0 \vartheta^n + f(|\psi_0^{n-1}|^2) \theta^n - f(|\Psi_0^{n-1}|^2) \Theta^n \right) \bar{\vartheta}^n - 3is_0^\alpha \vartheta^n \bar{\vartheta}^n - 8is_0^{3\alpha/2} \mathbf{e}^{-\frac{\pi}{4}i} e_0^n \bar{\vartheta}^n + iR_0^n \bar{\vartheta}^n \\
&+ (3s_0^{\frac{\alpha}{2}} \mathbf{e}^{-\frac{\pi}{4}i} e_J^n - \varphi^n) \bar{e}_J^n + \frac{h}{2} V_J e_J^n \bar{e}_J^n + \frac{h}{2} \left(f(|\psi_J^{n-1}|^2) \psi_J^n - f(|\Psi_J^{n-1}|^2) \Psi_J^n \right) \bar{e}_J^n + T_J^n \bar{e}_J^n \\
&+ \left[V_J \varphi^n + f(|\psi_J^{n-1}|^2) \phi^n - f(|\Psi_J^{n-1}|^2) \Phi^n \right] \bar{\varphi}^n - 3is_0^\alpha \varphi^n \bar{\varphi}^n + 8is_0^{\frac{3\alpha}{2}} \mathbf{e}^{-\frac{\pi}{4}i} e_J^n \bar{\varphi}^n + R_J^n \bar{\varphi}^n. \quad (4.33)
\end{aligned}$$

Now, we prove the results (4.25) and (4.26) by mathematical induction. First, we show that the estimates hold for $n = 1$. Since $\{\Psi_j^0, \Phi^0, \Theta^0\} = \{\psi_j^0, \phi^0, \theta^0\}$, we have

$$\left(f(|\psi_j^0|^2) \psi_j^1 - f(|\Psi_j^0|^2) \Psi_j^1 \right) \bar{e}_j^1 = \left(f(|\psi_j^0|^2) \psi_j^1 - f(|\psi_j^0|^2) \Psi_j^1 \right) \bar{e}_j^1 = f(|\psi_j^0|^2) |e_j^1|^2, \quad 0 \leq j \leq J, \quad (4.34)$$

$$\left(f(|\psi_0^0|^2) \theta^1 - f(|\Psi_0^0|^2) \Theta^1 \right) \bar{\vartheta}^1 = \left(f(|\psi_0^0|^2) \theta^1 - f(|\psi_0^0|^2) \Theta^1 \right) \bar{\vartheta}^1 = f(|\psi_0^0|^2) |\vartheta^1|^2, \quad (4.35)$$

$$\left(f(|\psi_J^0|^2) \phi^1 - f(|\Psi_J^0|^2) \Phi^1 \right) \bar{\varphi}^1 = \left(f(|\psi_J^0|^2) \phi^1 - f(|\psi_J^0|^2) \Phi^1 \right) \bar{\varphi}^1 = f(|\psi_J^0|^2) |\varphi^1|^2. \quad (4.36)$$

Thus, by taking the imaginary part of the equation (4.33) and by using the Cauchy-Schwarz inequality, we get

$$\Re \left((\mathcal{D}_\tau^\alpha e^1, e^1) + \bar{\varphi}^1 \mathcal{D}_\tau^\alpha \varphi^1 + \bar{\vartheta}^1 \mathcal{D}_\tau^\alpha \vartheta^1 \right) \leq C \|e^1\|^2 + C |\varphi^1|^2 + C |\vartheta^1|^2 + C(\tau + h^2)^2. \quad (4.37)$$

By Lemma 4.4, we conclude that there exists a parameter τ_1 such that, for $\tau \leq \tau_1$,

$$\|e^1\| + |\varphi^1| + |\vartheta^1| \leq C^*(\tau + h^2). \quad (4.38)$$

Meanwhile, we have

$$|e^1|_1^2 = h \sum_{j=1}^J |\delta_x \bar{e}_{j-\frac{1}{2}}^1| |\delta_x e_{j-\frac{1}{2}}^1| \leq h \sum_{j=1}^J \left(\frac{|e_j^1| + |e_{j-1}^1|}{h} \right)^2 \leq \frac{4}{h^2} \|e^1\|^2 \leq \frac{4C^*}{h^2} (\tau + h^2)^2. \quad (4.39)$$

Together with (4.38), (4.39) and Lemma 4.2, we deduce that

$$\|e^1\|_{L^\infty} \leq C(\tau + h^2 + \frac{\tau}{h}).$$

Hence, one obtains

$$\begin{aligned}
\|\Psi^1\|_\infty + |\Theta^1| + |\Phi^1| &\leq \|\psi^1\|_\infty + |\theta^1| + |\phi^1| + \|e^1\|_{L^\infty} + |\vartheta^1| + |\varphi^1| \\
&\leq \|\psi^1\|_\infty + |\theta^1| + |\phi^1| + C_1(\tau + h^2 + \frac{\tau}{h}) \leq K,
\end{aligned}$$

whenever $C_1(\tau + h^2 + \frac{\tau}{h}) \leq 1$.

Now, suppose that the main results (4.25) and (4.26) hold for $n \leq k-1$, then we have the following set of inequalities

$$\begin{aligned}
& \left(f(|\psi_j^{k-1}|^2)\psi_j^k - f(|\Psi_j^{k-1}|^2)\Psi_j^k \right) \\
&= \left(f(|\psi_j^{k-1}|^2)\psi_j^k - f(|\Psi_j^{k-1}|^2)\psi_j^k \right) + \left(f(|\Psi_j^{k-1}|^2)\psi_j^k - f(|\Psi_j^{k-1}|^2)\Psi_j^k \right) \\
&= \psi_j^k f'(\xi_j^{k-1})(|\psi_j^{k-1}|^2 - |\Psi_j^{k-1}|^2) + f(|\Psi_j^{k-1}|^2)(\psi_j^k - \Psi_j^k) \\
&\leq C(|e_j^{k-1}| + |e_j^k|),
\end{aligned} \tag{4.40}$$

where $\xi_j^{k-1} \in (\psi_j^{k-1}, \Psi_j^{k-1})$ and we remark that $\|\Psi_j^{k-1}\|_{L^\infty} \leq K$. Similarly, we show that

$$f(|\psi_0^{k-1}|^2)\theta^k - f(|\Psi_0^{k-1}|^2)\Theta^k \leq C|e_0^{k-1}| + C|\vartheta^k|, \tag{4.41}$$

$$f(|\psi_J^{k-1}|^2)\phi^k - f(|\Psi_J^{k-1}|^2)\Phi^k \leq C|e_J^{k-1}| + C|\varphi^k|. \tag{4.42}$$

In addition, we can write that

$$\begin{aligned}
& \Im \left((\vartheta^k + 3s_0^{\frac{\alpha}{2}} \mathbf{e}^{-\frac{\pi}{4}i} e_0^k) \bar{e}_0^k + T_0^k \bar{e}_0^k + (f(|\psi_0^{k-1}|^2)\theta^k - f(|\Psi_0^{k-1}|^2)\Theta^k) \bar{\vartheta}^k - 8is_0^{3\alpha/2} \mathbf{e}^{-\frac{\pi}{4}i} e_0^k \bar{\vartheta}^k \right) \\
&= -\frac{3\sqrt{2}}{2} s_0^{\frac{\alpha}{2}} |e_0^k|^2 + \Im \left(\vartheta^k \bar{e}_0^k + T_0^k \bar{e}_0^k + (f(|\psi_0^{k-1}|^2)\theta^k - f(|\Psi_0^{k-1}|^2)\Theta^k) \bar{\vartheta}^k - 8is_0^{3\alpha/2} \mathbf{e}^{-\frac{\pi}{4}i} e_0^k \bar{\vartheta}^k \right) \\
&\leq -\frac{3\sqrt{2}}{2} s_0^{\frac{\alpha}{2}} |e_0^k|^2 + \left(C_1 |\bar{e}_0^k|^2 + \frac{1}{4C_1} |\vartheta^k|^2 \right) + \left(C_2 |\bar{e}_0^k|^2 + \frac{1}{4C_2} |T_0^k|^2 \right) + \left(C_3 |e_0^k|^2 + \frac{1}{4C_3} |\vartheta^k|^2 \right) \\
&\quad + \Re(8is_0^{3\alpha/2} \mathbf{e}^{-\frac{\pi}{4}i}) \left(C_4 |\bar{e}_0^k|^2 + \frac{1}{4C_4} |\vartheta^k|^2 \right),
\end{aligned}$$

where C_i , $i = 1, 2, 3, 4$ are arbitrary positive real-valued constants. Let us set $C_1 + C_2 + C_3 + \Re(8is_0^{3\alpha/2})C_4 = 3\sqrt{2}s_0^{\frac{\alpha}{2}}/2$ in the above formula. We then deduce that

$$\begin{aligned}
& \Im \left((\vartheta^k + 3s_0^{\frac{\alpha}{2}} \mathbf{e}^{-\frac{\pi}{4}i} e_0^k) \bar{e}_0^k + T_0^k \bar{e}_0^k + (f(|\psi_0^{k-1}|^2)\theta^k - f(|\Psi_0^{k-1}|^2)\Theta^k) \bar{\vartheta}^k - 8is_0^{3\alpha/2} \mathbf{e}^{-\frac{\pi}{4}i} e_0^k \bar{\vartheta}^k \right) \\
&\leq C|\vartheta^k|^2 + C|T_0^k|^2.
\end{aligned} \tag{4.43}$$

Similarly to (4.43), we obtain

$$\begin{aligned}
& \Im \left((3s_0^{\frac{\alpha}{2}} \mathbf{e}^{-\frac{\pi}{4}i} e_J^n - \varphi^n) \bar{e}_J^n + T_J^n \bar{e}_J^n + (f(|\psi_J^{n-1}|^2)\phi^n - f(|\Psi_J^{n-1}|^2)\Phi^n) \bar{\varphi}^n + 8is_0^{\frac{3\alpha}{2}} \mathbf{e}^{-\frac{\pi}{4}i} e_J^n \bar{\varphi}^n \right) \\
&\leq C|\varphi^n|^2 + C|T_J^n|^2.
\end{aligned} \tag{4.44}$$

Now, let us consider $n = k$ in (4.33). By taking the imaginary part of the resulting equation, by using (4.40)-(4.44) and the Cauchy-Schwarz inequality, one gets

$$\Re \left(({}_0^C \mathbb{D}_\tau^\alpha e^k, e^k) + \bar{\varphi}^k {}_0^C \mathbb{D}_\tau^\alpha \varphi^k + \bar{\vartheta}^k {}_0^C \mathbb{D}_\tau^\alpha \vartheta^k \right) \tag{4.45}$$

$$\leq C \left(\|e^{k-1}\|^2 + \|e^k\|^2 + |\varphi^k|^2 + |\vartheta^k|^2 + (\tau + h^2)^2 \right). \tag{4.46}$$

Now, by Lemma 4.4, when $\tau < \tau_2$, we prove that there exists a parameter τ_2 such that

$$\|e^k\| + |\varphi^k| + |\vartheta^k| \leq C^*(\tau + h^2). \tag{4.47}$$

Moreover, we have

$$|e^k|_1^2 = h \left| \sum_{j=1}^J (\delta_x \bar{e}_{j-\frac{1}{2}}^k) (\delta_x e_{j-\frac{1}{2}}^k) \right| \leq \frac{4}{h^2} \|e^k\|^2 \leq \frac{4C^*}{h^2} (\tau + h^2)^2. \quad (4.48)$$

Together with (4.47), (4.48) and Lemma 4.2, we deduce that

$$\|e^k\|_{L^\infty} \leq C(\tau + h^2 + \frac{\tau}{h}).$$

Therefore, we obtain

$$\begin{aligned} \|\Psi^k\|_\infty + |\Theta^k| + |\Phi^k| &\leq \|\psi^k\|_\infty + |\theta^k| + |\phi^k| + \|e^k\|_{L^\infty} + |\vartheta^k| + |\vartheta^k| \\ &\leq \|\psi^k\|_\infty + |\theta^k| + |\phi^k| + C(\tau + h^2 + \frac{\tau}{h}) \leq K, \end{aligned}$$

as long as $C_2(\tau + h^2 + \frac{\tau}{h}) \leq 1$. Finally, the conclusions also hold for $n = k$, completing hence the proof. \blacksquare

4.3 Fast evaluation based on the L1-schemes

We now introduce the fast evaluation of the Caputo derivative, proposed in [27], to circumvent the huge storage and computational cost for the long time simulation. The main idea of this fast evaluation algorithm is to split the Caputo derivative into the sum of a local part and a history part

$${}_0^C \mathcal{D}_t^\alpha \psi^n = \frac{1}{\Gamma(1-\alpha)} \int_{t_{n-1}}^{t_n} \frac{\psi'(x, s) ds}{(t_n - s)^\alpha} + \frac{1}{\Gamma(1-\alpha)} \int_0^{t_{n-1}} \frac{\psi'(s) ds}{(t_n - s)^\alpha} := C_{\text{loc}}(t_n) + C_{\text{hist}}(t_n).$$

For the local part $C_{\text{loc}}(t_n)$, we apply the L1-approximation, i.e.,

$$C_{\text{loc}}(t_n) \approx \frac{\psi(x, t_n) - \psi(x, t_{n-1})}{\tau \Gamma(1-\alpha)} \int_{t_{n-1}}^{t_n} \frac{1}{(t_n - s)^\alpha} ds = \frac{\psi(x, t_n) - \psi(x, t_{n-1})}{\tau^\alpha \Gamma(2-\alpha)}. \quad (4.49)$$

For the history part $C_{\text{hist}}(t_n)$, we integrate by part and get

$$C_{\text{hist}}(t_n) = \frac{1}{\Gamma(1-\alpha)} \left[\frac{\psi(x, t_{n-1})}{\tau^\alpha} - \frac{\psi(x, t_0)}{t_n^\alpha} - \alpha \int_0^{t_{n-1}} \frac{\psi(x, s) ds}{(t_n - s)^{1+\alpha}} \right]. \quad (4.50)$$

Then, we use a sum-of-exponentials expansion to approximate the convolution integral of ψ^n with the kernel $t^{-1-\alpha}$. For a given absolute error ε and for α , there exist some positive real numbers s_i and w_i , $i = 1, \dots, N_{\text{exp}}$ (N_{exp} is the number of exponentials) such that

$$\left| \frac{1}{t^{1+\alpha}} - \sum_{i=1}^{N_{\text{exp}}} \omega_i e^{-s_i t} \right| \leq \varepsilon, \quad \text{for all } t \in [\tau, T]. \quad (4.51)$$

We replace the kernel $\frac{1}{t^{1+\alpha}}$ in (4.50) by its sum-of-exponentials approximation in (4.51) to have

$$C_{\text{hist}}(t_n) \approx \frac{1}{\Gamma(1-\alpha)} \left[\frac{\psi(x, t_{n-1})}{\tau^\alpha} - \frac{\psi(x, t_0)}{t_n^\alpha} - \alpha \sum_{i=1}^{N_{\text{exp}}} \omega_i U_{\text{hist}, i}(t_n) \right],$$

where $U_{\text{hist},i}(t_n)$ is defined by

$$U_{\text{hist},i}(t_n) = \int_0^{t_{n-1}} e^{-(t_n-s)s_i} \psi(x, s) ds,$$

and has a simple recurrence relation

$$U_{\text{hist},i}(t_n) = e^{-s_i \tau} U_{\text{hist},i}(t_{n-1}) + \int_{t_{n-2}}^{t_{n-1}} e^{-s_i(t_n-s)} \psi(x, s) ds, \quad (4.52)$$

with $U_{\text{hist},i}(t_0) = 0$. The integral can be calculated by

$$\int_{t_{n-2}}^{t_{n-1}} e^{-s_i(t_n-s)} \psi(x, s) ds \approx \frac{e^{-s_i \tau}}{s_i^2 \tau} [(e^{-s_i \tau} - 1 + s_i \tau) \psi^{n-1} + (1 - e^{-s_i \tau} - e^{-s_i \tau} s_i \tau) \psi^{n-2}].$$

Finally, the Fast approximate evaluation of the Caputo fractional derivative is given by

$${}^F C \mathbb{D}_t^\alpha \psi^n = \frac{\psi(x, t_n) - \psi(x, t_{n-1})}{\tau^\alpha \Gamma(2-\alpha)} + \frac{1}{\Gamma(1-\alpha)} \left[\frac{\psi(x, t_{n-1})}{\tau^\alpha} - \frac{\psi(x, t_0)}{t_n^\alpha} - \alpha \sum_{i=1}^{N_{\text{exp}}} \omega_i U_{\text{hist},i}(t_n) \right], \quad (4.53)$$

for $n > 0$, and where $U_{\text{hist},i}(t_n)$ can be obtained by the recurrence relation (4.52).

The following lemma provides an error bound for the fast approximation ${}^F C \mathbb{D}_t^\alpha \psi^n$ appearing in (4.53).

Lemma 4.6 (see [27]) *We assume that $\psi(t) \in C^2([0, t_n])$ and let*

$${}^F R^n \psi := {}^C D_t^\alpha \psi(x, t)|_{t=t_n} - {}^F C \mathbb{D}_t^\alpha \psi^n(x, t_n), \quad \text{with } 0 < \alpha < 1.$$

Then, we have the following error inequality

$$|{}^F R^n \psi| \leq \frac{\tau^{2-\alpha}}{\Gamma(2-\alpha)} \left(\frac{1-\alpha}{12} + \frac{2^{2-\alpha}}{2-\alpha} - (1+2^{-\alpha}) \right) \max_{0 \leq t \leq t_n} |\psi''(x, t)| + \frac{\alpha \varepsilon t_{n-1}}{\Gamma(1-\alpha)} \max_{0 \leq t \leq t_{n-1}} |\psi(x, t)|.$$

By using the fast evaluation of the Caputo derivative instead of the direct L1-approximation in (4.14)-(4.19), we have the finite difference scheme given by

$$i_0^F C \mathbb{D}_t^\alpha \Psi_j^n = -\delta_x^2 \Psi_j^n + [V_j + f(|\Psi_j^{n-1}|^2)] \Psi_j^n, \quad 1 \leq j \leq J-1, 1 \leq n \leq N, \quad (4.54)$$

$$i_{\frac{h}{2}}^F C \mathbb{D}_t^\alpha \Psi_0^n = -\delta_x \Psi_{\frac{1}{2}}^n + (\Theta^n - 3s_0^{\frac{\alpha}{2}} e^{-\frac{\pi i}{4}} \Psi_0^n) + \frac{h}{2} [V_0 + f(|\Psi_0^{n-1}|^2)] \Psi_0^n, \quad (4.55)$$

$${}^F C \mathbb{D}_t^\alpha \Theta^n = -i [V_0 + f(|\Psi_0^{n-1}|^2)] \Theta^n + 3s_0^\alpha \Theta^n + 8s_0^{\frac{3\alpha}{2}} e^{-\frac{\pi i}{4}} \Psi_0^n, \quad (4.56)$$

$$i_{\frac{h}{2}}^F C \mathbb{D}_t^\alpha \Psi_J^n = \delta_x \Psi_{J-\frac{1}{2}}^n + (3s_0^{\frac{\alpha}{2}} e^{-\frac{\pi i}{4}} \Psi_J^n - \Phi^n) + \frac{h}{2} [V_J + f(|\Psi_J^{n-1}|^2)] \Psi_J^n, \quad (4.57)$$

$${}^F C \mathbb{D}_t^\alpha \Phi^n = -i [V_J + f(|\Psi_J^{n-1}|^2)] \Phi^n + 3s_0^\alpha \Phi^n - 8s_0^{\frac{3\alpha}{2}} e^{-\frac{\pi i}{4}} \Psi_J^n, \quad (4.58)$$

$$\Psi_j^0 = \Psi_0(x_j), \quad 0 \leq j \leq J. \quad (4.59)$$

Furthermore, the error estimate is given as follows.

Theorem 4.7 *Let us suppose that (3.1)-(3.4) has a unique smooth solution $(\psi(x, t), \theta(t), \phi(t))$ in $\Omega^{int} \times [0, T]$. Then, there exist some positive real-valued constants τ_0 and h_0 such that, for $\tau \leq \tau_0$ and $h \leq h_0$, the system (4.54)-(4.59) admits a unique solution $\{\Psi_j^n, \Phi^n, \Theta^n\}$, $n = 1, 2, \dots, N$, satisfying*

$$\|\Psi^n\|_\infty + |\Theta^n| + |\Phi^n| \leq K, \quad (4.60)$$

$$\|e^n\| + |\varphi^n| + |\vartheta^n| \leq C_1^*(\tau + h^2 + \epsilon). \quad (4.61)$$

The proof of (4.61) is similar to the one of (4.26) by using the truncation error given in Lemma 4.6.

5 Numerical examples

In this section, we provide four examples to not only demonstrate the effectiveness of our method, but also to illustrate the dynamics of numerical solutions of TFNSEs in different situations.

Example 1. In this example we consider the TFNSE with cubic nonlinearity, i.e. $f(|\psi|) = 2|\psi|^2$ and with the gaussian potential $V(x) := e^{-5x^2}$. The initial data is: $\psi_0(x) = e^{-5x^2}$. For the calculations in Figures 1 and 2, we fix : $T = 4$ and $]x_\ell, x_r[:=]-5, 5[$. The left and right pictures represent the amplitude of the wave field, i.e. $|\psi_{\tau, h}^{\alpha, \text{fast}}|$, for $\alpha = 0.5$ and $\alpha = 0.75$, respectively, and computed by the fast scheme (4.54)-(4.59) for the discretization parameters $\tau := T/N = 10^{-3}$ ($N = 4 \times 10^3$) and $h := (x_r - x_\ell)/J = 5 \times 10^{-2}$ ($J = 200$), with the tolerance parameter $\epsilon = 10^{-9}$. For the ABCs, we fix $s_0 = 20$ (we see below that any other value s_0 does not modify the results). The CPU time for $\alpha = 0.5$ is 21 (sec.) and 27 (sec.) for $\alpha = 0.75$. Using the fast scheme compared with the direct scheme (4.14)-(4.19) does not affect the accuracy. Indeed, we report on Figure 2 the absolute error between $\psi_{\tau, h}^{\alpha, \text{fast}}$ and $\psi_{\tau, h}^{\alpha, \text{dir}}$ ("dir" means "direct" here): $|\psi_{\tau, h}^{\alpha, \text{fast}} - \psi_{\tau, h}^{\alpha, \text{dir}}|$, on the grid for the same discretization parameters τ and h , and the two values of α . The error is smaller than ϵ and clearly does not modify the accuracy of a given computation. To demonstrate the complexity of the two schemes (direct vs. fast), we plot on Figure 3 the CPU time of the two schemes in seconds vs. the number N of grid points in time. We observe that while the CPU time for the direct scheme scales as $\mathcal{O}(N^2)$, it increases almost linearly with respect to N for the fast scheme. There is a significant speed-up even for moderate values of N .

From these first computations, we conclude that the fast scheme leads to a similar accuracy as for the direct scheme (according to the tolerance ϵ , other computations confirming this observation) while being much more efficient, with a nearly linear cost in time for a low storage, most particularly when τ gets smaller. For these reasons, we now always use the fast scheme to study the convergence rates in space and time, and for the various simulations. We also denote $\psi_{\tau, h}^{\alpha, \text{fast}}$ by $\psi_{\tau, h}$ to simplify the notations in the text (but we keep the initial notation $\psi_{\tau, h}^{\alpha, \text{fast}}$ inside the figures).

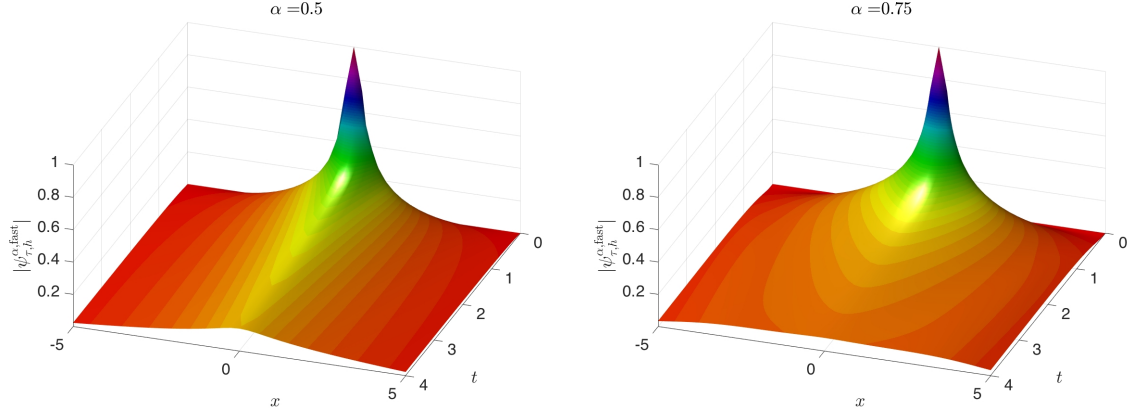


Figure 1: **(Example 1)** amplitude $|\psi_{\tau,h}^{\alpha,\text{fast}}|$ for $\alpha = 0.5$ (left) and $\alpha = 0.75$ (right).

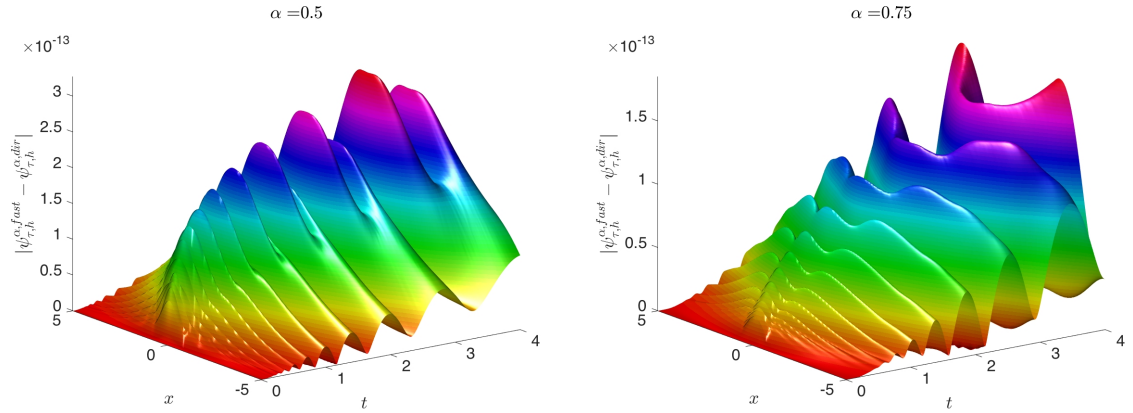


Figure 2: **(Example 1)** absolute error $|\psi_{\tau,h}^{\alpha,\text{fast}} - \psi_{\tau,h}^{\alpha,\text{dir}}|$ for $\alpha = 0.5$ (left) and $\alpha = 0.75$ (right).

We now analyze both the truncation error related to the introduction of an ABC and the convergence rate of the fast scheme. To this aim, we compute a reference solution ψ^{ref} on the larger domain $]-12, 12[$ until the time $T = 0.5$, for some extremely small values of τ and h . We report the following error: we define $E_\infty(N, J) := \|\psi^{\text{ref}} - \psi_{\tau,h}\|_\infty$ for two fixed values of τ and h . When analyzing the convergence rate in space of the fast scheme, we represent the quantity $E_\infty(N_0, J) := \|\psi^{\text{ref}} - \psi_{\tau_0,h}\|_\infty$ vs. J (both in \log_{10} -scale) for $\tau_0 = 10^{-4}$ ($N_0 = 5 \times 10^3$) and for various values of s_0 . When we study the convergence rate in time, we fix $h_0 := 5 \times 10^{-3}$ ($J_0 = 2 \times 10^3$) and represent $E_\infty(N, J_0) := \|\psi^{\text{ref}} - \psi_{\tau,h_0}\|_\infty$ vs. N (in \log_{10} -scale). From Figures 4 and 5, we show that both the convergence rate of the fast scheme (4.54)–(4.59) (as well as direct scheme (4.14)–(4.19)) is of the order of $\mathcal{O}(h^2 + \tau)$. In addition, the ABCs are accurate and not affected by the choice of the parameter s_0 . Finally, an analysis (not reported here) shows that the L_∞ -error of the direct and fast schemes is almost the same (up to the tolerance ε).

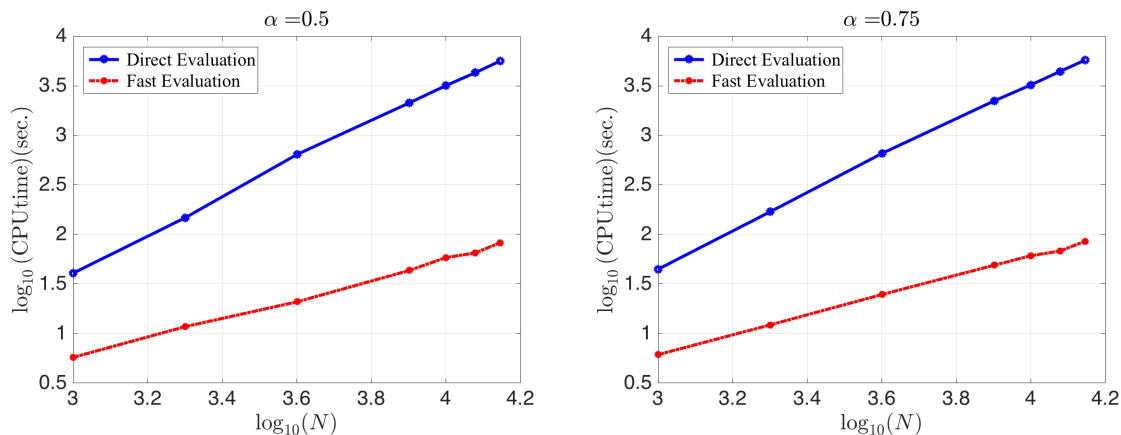


Figure 3: **(Example 1)** comparison of the CPU time (sec. in \log_{10} -scale) required for the direct and fast methods vs. the number N of time points (\log_{10} scale) (left: $\alpha = 0.5$; right: $\alpha = 0.75$).

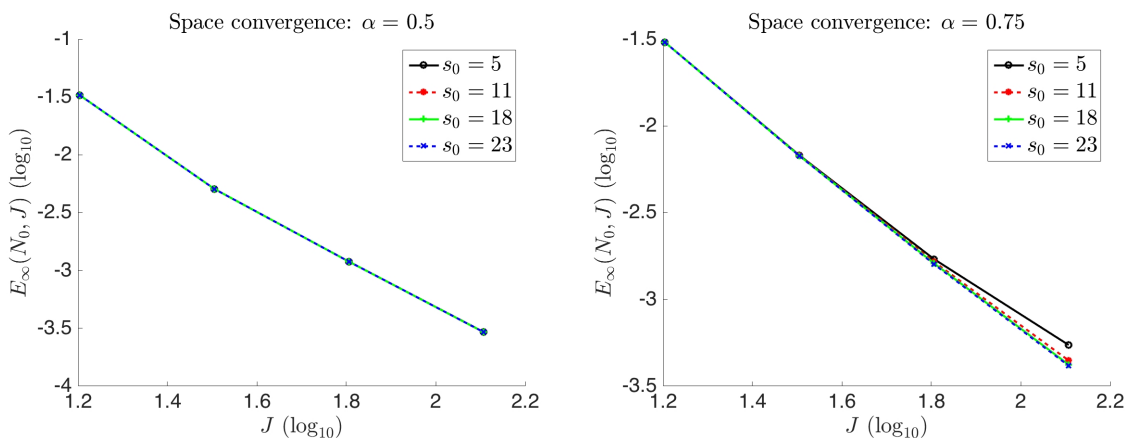


Figure 4: **(Example 1)** $E_{\infty}(N_0, J)$ vs. J (both in \log_{10} -scale) for various values of s_0 and by using the fast scheme (4.54)-(4.59) (left: $\alpha = 0.5$; right: $\alpha = 0.75$).

Example 2. In this second example, we investigate the evolution of the numerical solution ψ of the TFNSE for different fractional orders α with the nonlinearity $f(|\psi|^2)\psi = -2|\psi|^2\psi$ and for $V(x) = 0$. The initial data is $\psi_0 = e^{2i(x+3)}\text{sech}(x+3)$. The computational domain is $] -10, 10[$ for a maximal time of computation $T = 2$. The discretization parameters are $\tau = 4 \times 10^{-3}$ ($N = 5 \times 10^2$) and $h = 2 \times 10^{-2}$ ($J = 10^3$). For the ABC, we consider $s_0 = 20$.

In the standard situation, i.e. for $\alpha = 1$, the soliton propagates from the left to the right domain with a given angle. One can see on Figure 6 that the evolution of the solution is pretty sharp on the first time steps and then the solution propagates straight when $\alpha = 0.25$ with less dispersion. The situation tends to the standard case when α tends to 1.

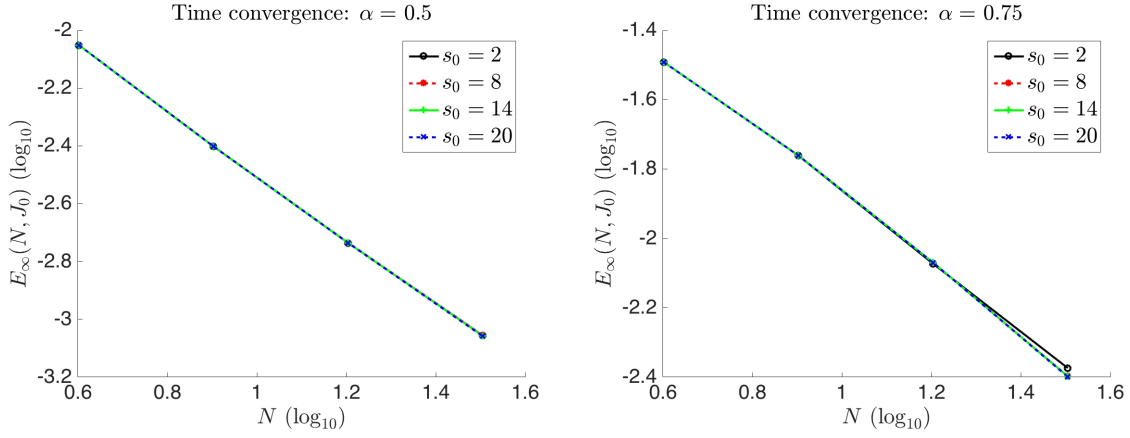


Figure 5: (**Example 1**) $E_\infty(N, J_0)$ vs. N (both in \log_{10} -scale) for various values of s_0 and by using the fast scheme (4.54)-(4.59) (left: $\alpha = 0.5$; right: $\alpha = 0.75$).

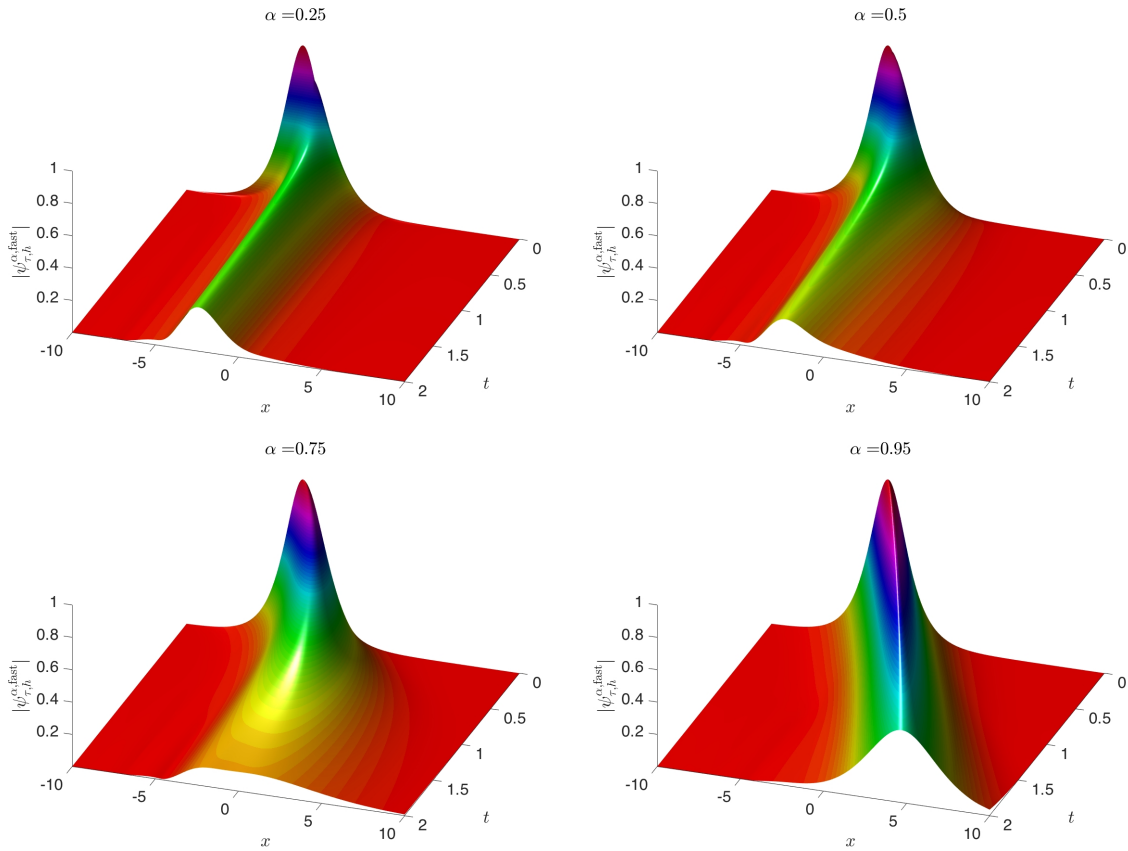


Figure 6: (**Example 2**) evolution of $|\psi|$ for $\alpha = 0.25$ (CPU time 87 sec.), 0.5 (89 sec.), 0.75 (85 sec.) and 0.95 (76 sec.).

Example 3. This third example, reported on Figure 7, is dedicated to the collision of two waves for different values of α . The nonlinearity and the external potential for the TFNSE are respectively given by

$$f(|\psi|^2)\psi = -2|\psi|^2\psi, \quad V(x) = e^{-3x^2}.$$

The initial data is built as the superposition of two waves

$$\psi_0(x) = e^{-2i(x-8)}\text{sech}(x-8) + e^{2i(x+8)}\text{sech}(x+8).$$

We consider the interval $] -20, 20[$ and a final computational time $T = 6$. We fix $N = 3000$ grid points in time and $J = 1000$ spatial discrete points. For the ABC, we choose $s_0 = 20$.

For the standard nonlinear equation with $\alpha = 1$, the two soliton waves collide and keep their own shapes moving away after the collision. This can be observed here when α is close to 1. For smaller values of α , this property is lost and the waves do not even cross. At the same time, some waves are created, with high oscillations corresponding to fluctuations and suggesting the appearance of a decoherence phenomena that depends on α .

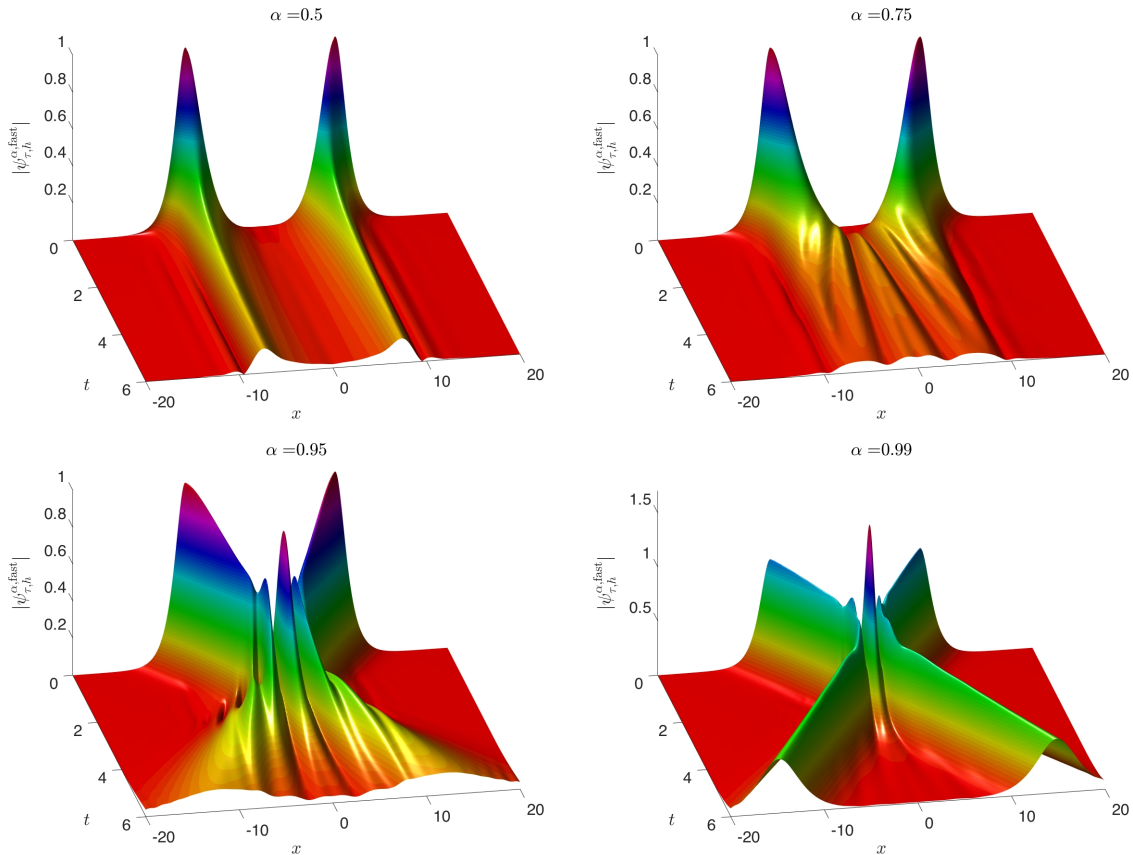


Figure 7: (**Example 3**) evolution of $|\psi|$ for $\alpha = 0.5$ (487 sec.), 0.75 (442 sec.), 0.95 (540 sec.) and 0.999 (545 sec.).

Example 4. In this last example, we consider the TFNSE with a cubic-plus-quintic nonlinearity $f(|\psi|^2)\psi = 2|\psi|^2\psi + |\psi|^4\psi$ and $V(x) = 0$. The initial data is built as the superposition of two Gaussian functions

$$\psi_0 = e^{-3(x-2)^2} + e^{-3(x+2)^2}.$$

The interval of computation is $]-15, 15[$ and the final time is $T = 3$. The time step is $\tau = 4 \times 10^{-3}$ (for $N = 750$ points) and the spatial mesh size is equal to $h = 1.5 \times 10^{-2}$ (with $J = 2 \times 10^3$ points). For the ABC, we consider $s_0 = 20$.

The dynamics of the solution is plotted on Figure 8 for various values of α . While the two waves clearly mixed for α close to 1 with many oscillations and then largely spread out, they tend to form just one smooth wave after a short time, propagating without being deformed. The support tends to be smaller when α decays.

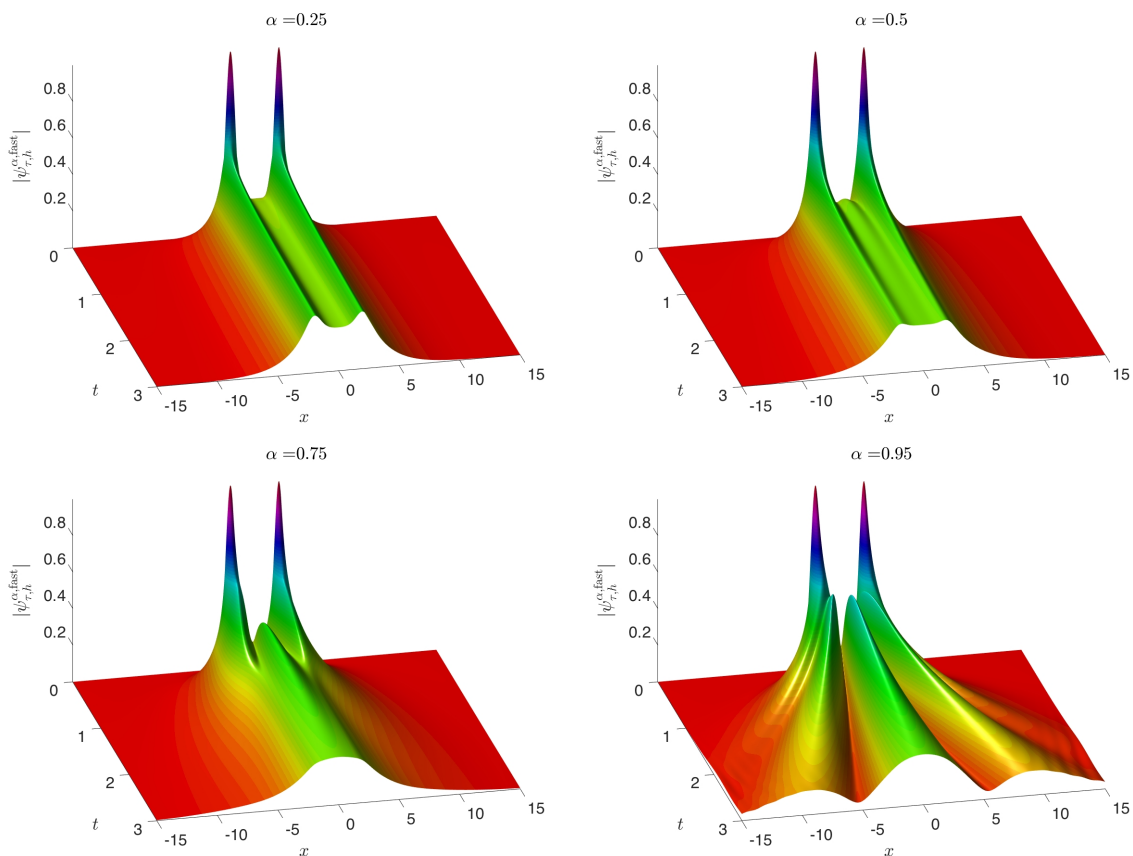


Figure 8: (**Example 4**) evolution of $|\psi|$ for $\alpha = 0.25$ (717 sec.), 0.5 (627 sec.), 0.75 (668 sec.) and 0.95 (645 sec.).

6 Conclusion

In this paper, we studied the computation of the time fractional nonlinear Schrödinger equation (TFNSE) on unbounded domain. First, we generalized the construction of approximate non-

linear ABCs through the unified approach proposed in [57, 58] to compute the solution to the TFNSE. In addition, we analyzed the stability of the reduced problem with the approximate nonlinear ABCs and the convergence of the linearized finite difference scheme. To speed-up the computations, we used the fast evaluation of the fractional Caputo derivative given in [27]. We presented some numerical examples to verify the performance of the proposed numerical methods. The extension of the method to the two-dimensional TFNSE on unbounded domain and its fast evaluation will be discussed in a future work.

References

- [1] X. Antoine, A. Arnold, C. Besse, M. Ehrhardt and A. Schädle, A review of transparent and artificial boundary conditions techniques for linear and nonlinear Schrödinger equations, *Commun. Comput. Phys.*, 4 (4) (2008), 729-796.
- [2] X. Antoine, W. Bao and C. Besse, Computational methods for the dynamics of the nonlinear Schrödinger/Gross-Pitaevskii equations, *Comput. Phys. Commun.* 184 (12), (2013), 2621-2633.
- [3] X. Antoine, C. Besse and P. Klein, Absorbing boundary conditions for the one-dimensional Schrödinger equation with an exterior repulsive potential, *J. Comput. Phys.*, 228(2) (2009), 312-335.
- [4] X. Antoine, C. Besse and P. Klein, Absorbing boundary conditions for general nonlinear Schrödinger equations, *SIAM J. Sci. Comput.*, 33 (2) (2011), 1008-1033.
- [5] X. Antoine, C. Besse and P. Klein, Absorbing boundary conditions for the two-dimensional Schrödinger equation with an exterior potential. Part II: discretization and numerical results, *Numer. Math.*, 125 (2013), 191-223.
- [6] X. Antoine, E. Lorin and Q. Tang, A friendly review of absorbing boundary conditions and perfectly matched layers for classical and relativistic quantum waves equations, to appear in *Molecular Phys.*, 2017.
- [7] X. Antoine, Q. Tang and Y. Zhang, On the ground states and dynamics of space fractional nonlinear Schrödinger/Gross-Pitaevskii equations with rotation term and nonlocal nonlinear interactions, *J. Comput. Phys.*, 325 (2016), 74-97.
- [8] A.A. Awotunde, R.A. Ghanam, N. Tatar, Artificial boundary condition for a modified fractional diffusion problem, *Bound. Value Probl.*, 1 (2015), 1-17.
- [9] G.A. Baker, and P. Graves-Morris, *Padé Approximations*, 2nd edition, Cambridge University Press, 1996.
- [10] A. Bamberger, B. Engquist, L. Halpern and P. Joly, Higher order paraxial wave equation approximations in heterogeneous media, *SIAM J. Appl. Math.*, 48 (1988), 129-154.
- [11] W. Bao and Y. Cai, Mathematical theory and numerical methods for Bose-Einstein condensation, *Kinet. Relat. Mod.*, Vol. 6 (2013), 1-135.

- [12] M. Bhatti, Fractional Schrödinger wave equation and fractional uncertainty principle, International J. Contem. Math. Sci., 2 (2007), 943-950.
- [13] A.H. Bhrawy and M.A. Abdelkawy, A fully spectral collocation approximation for multi-dimensional fractional Schrödinger equations, J. Comput. Phys., 294 (2015), 462-483.
- [14] H. Brunner, H. Han and D. Yin, Artificial boundary conditions and finite difference approximations for a time-fractional diffusion-wave equation on a two-dimensional unbounded spatial domain, J. Comput. Phy., 276 (2014), 541-562.
- [15] J. Cao and C. Xu, A high order scheme for the numerical solution of the fractional ordinary differential equations, J. Comput. Phys., 238 (2013), 154-168.
- [16] W. Cao, Z. Zhang and G. Karniadakis, Time-splitting schemes for fractional differential equations I: smooth solutions, SIAM J. Sci. Comput., 37(4) (2015), A1752-A1776.
- [17] J. Dea, Absorbing boundary conditions for the fractional wave equation, Appl. Math. Comput. 219 (2013), 9810-9820.
- [18] J. Dong and M. Xu, Space-time fractional Schrödinger equation with time-independent potentials, J. Math. Anal. Appl., 344(2)(2008), 1005-1017.
- [19] S. Duo and Y. Zhang, Computing the ground and first excited states of fractional Schrödinger equations in an infinite potential well, Commun. Comput. Phys., 18 (2015), 321-350.
- [20] B. Engquist and A. Majda, Absorbing boundary conditions for the numerical simulation of waves, Math. Comp., 31 (1977), 629-357.
- [21] G. H. Gao and Z. Z. Sun, A new fractional numerical differentiation formula to approximate the Caputo fractional derivative and its applications, J. Comput. Phys., 259 (2014), 33–50.
- [22] R. Garrappa, I. Moret and M. Popolizio, Solving the time-fractional Schrödinger equation by Krylov projection methods, J. Comput. Phys. 293 (2015), 115-134.
- [23] R. Ghaffari and S.M. Hosseini, Obtaining artificial boundary conditions for fractional sub-diffusion equation on space two-dimensional unbounded domains. Comput. Math. Appl., 68(1) (2014), 13-26.
- [24] B. Guo and Z. Huo, Well-posedness for the nonlinear fractional Schrödinger equation and inviscid limit behavior of solution for the fractional Ginzburg-Landau equation, Fract. Cal. and Appl. Anal., 16(1)(2013), 226-242.
- [25] H. Han, X. Wu, *Artificial Boundary Method*, Tsinghua Univ. Press, 2013.
- [26] B. Hicdurmaz and A. Ashyralyev, A stable numerical method for multidimensional time fractional Schrödinger equation, Comput. Math. Appl., 72 (2016), 1703-1713.
- [27] S. Jiang, J. Zhang, Q. Zhang and Z. Zhang, Fast evaluation of the Caputo fractional derivative and its applications to fractional diffusion equations. To appear in Commun. Comput. Phys., <http://arxiv.org/abs/1511.03453>.

- [28] W. Jones and W. Thron, *Continued Fractions, Analytic Theory and Applications*, Addison-Wesley Publishing Company, 1980.
- [29] N. Khan, M. Jamil and A. Ara, Approximate solutions to time-fractional Schrödinger equation via homotopy analysis method, *ISRN Math. Phys.*, 2012, Article ID 197068.
- [30] J. Kuska, Absorbing boundary conditions for the Schrödinger equation on finite intervals, *Phys. Rev. B*, 46(1992), 5000.
- [31] D. Kusnezov, A. Bulgac, and G. Dang, Quantum Lévy processes and fractional kinetics, *Phys. Rev. Lett.*, 82 (1999), 1136.
- [32] T. Langlands and B. Henry, The accuracy and stability of an implicit solution method for the fractional diffusion equation, *J. Comput. Phys.*, 205 (2005), 719-736.
- [33] N. Laskin, Fractional quantum mechanics, *Phys. Rev. E*, 62(2000), 3135-3145.
- [34] N. Laskin, Fractional quantum mechanics and Lévy path integrals. *Phys. Lett. A*, 268 (2000), 298-304.
- [35] N. Laskin, Fractional Schrödinger equation, *Phys. Rev. E*, 66 (2002), 056108.
- [36] N. Laskin, Fractals and quantum mechanics. *Chaos*, 10 (2000), 780-790.
- [37] C. Li, A. Chen, and J. Ye, Numerical approaches to fractional calculus and fractional ordinary differential equation, *J. Comput. Phys.*, 230 (2011), 3352-3368.
- [38] C. Li, W. Deng, and Y. Wu, Numerical analysis and physical simulations for the time fractional radial diffusion equation, *Comput. Math. Appl.*, 62 (2011), 1024-1037.
- [39] D. Li, H. Liao, W. Sun, J. Wang, J. Zhang, Analysis of L1-Galerkin FEMs for time-fractional parabolic problems, submitted.
- [40] Y. Lin and C. Xu, Finite difference/spectral approximations for time-fractional diffusion equation, *J. Comput. Phys.*, 225 (2007), 1533-1552.
- [41] A. Lomin, Fractional-time quantum dynamics, *Phys. Rev. E*, 62 (2000), 3135-3145.
- [42] A. Lonescu and F. Pusateri, Nonlinear fractional Schrödinger equations in one dimension, *J. Funct. Anal.*, 266(1)(2014), 139-176.
- [43] Y.Y. Lu, A Padé approximation method for square roots of symmetric positive definite matrices, *SIAM J. Math. Anal. Appl.*, 19(3)(1998), 833-845.
- [44] A. Mohebbi, M. Abbaszadeh and M. Dehghan, The use of a meshless technique based on collocation and radial basis functions for solving the time fractional nonlinear Schrödinger equation arising in quantum mechanics, *Engineering Analysis with Boundary Elements*, 37 (2013), 475-485.
- [45] M. Naber, Time fractional Schrödinger equation, *J. Math. Phys.*, 45 (2004), 3339-3352.
- [46] B. Narahari Achar, Bradley T. Yale, and John W. Hanneken, Time fractional Schrödinger equation revisited, *Adv. Math. Phys.*, (2013) Article ID 290216.

- [47] Z. Odibat, Approximations of fractional integrals and Caputo fractional derivatives, *Appl. Math. Comput.*, 178 (2006), 527-533.
- [48] Z. Odibat, S. Momani, and A. Alawneh, Analytic study on time-fractional Schrödinger equations: exact solutions by GDTM, *J. Phys.: Conference Series* 96 (2008), 012066.
- [49] I. Podlubny, *Fractional Differential Equations*, Academic Press, San Diego, 1999.
- [50] H. Spohn, Kinetic equations from Hamiltonian dynamics: Markovian limits, *Rev. Mod. Phys.* 52(1980), 569-615.
- [51] Z. Sun and X. Wu, A fully discrete difference scheme for a diffusion-wave system, *Appl. Numer. Math.*, 56 (2006), 193-209.
- [52] V. Tarasov, Fractional Heisenberg Equation, *Phys. Lett. A*, 372 (2006), 2984-2988.
- [53] S. Wang and M. Xu, Generalized fractional Schrödinger equation with space-time fractional derivatives, *J. Math. Phys.*, 48(4) (2007), 043502.
- [54] L. Wei, Y. He, X. Zhang and S. Wang, Analysis of an implicit fully discrete local discontinuous Galerkin method for the time-fractional Schrödinger equation, *Finite Elements in Analysis and Design*, 59 (2012), 28-34.
- [55] B. West, Quantum Lévy propagators, *J. Phys. Chem. B*, 104 (2000), 3830-3832.
- [56] B. West, M. Bologna, and P. Grigolini, *Physics of Fractal Operators*, Springer, New York, 2002.
- [57] J. Zhang, Z. Xu, X. Wu, Unified approach to split absorbing boundary conditions for nonlinear Schrödinger equations, *Phys. Rev. E*, 78 (2008), 026709.
- [58] J. Zhang, Z. Xu, X. Wu, Unified approach to split absorbing boundary conditions for nonlinear Schrödinger equations: Two dimensional case, *Phys. Rev. E*, 79 (2009), 046711.
- [59] I. Podlubny, *Fractional Differential Equations*, Academic Press, San Diego, 1999.
- [60] J. Zhang, Z. Xu, X. Wu and D. Wang, Stability analysis of local absorbing boundary conditions for general nonlinear Schrödinger equations in one and two dimensions, to appear in *J. Comput. Math.* 2016.